An Abstract Of The Thesis Of

James R. LaFortune for the degree of Master of Science in Geology presented on May 20, 1988 . Title: Geology and Geochemistry of Indian Plate Rocks South of the Indus Suture, Besham Area, Northern Pakistan .

Redacted for privacy

Abstract approved: _____
Dr. Lawrence W. Snee

The Himalaya are the geologic manifestation of continental collision, and in northern Pakistan the Main Mantle thrust (MMT) is a major suture along which the collision occurred. A newly recognized basement uplift near Besham village in southern Kohistan, adjacent to the MMT, is bounded on the east and west by north-trending high angle fault zones. The uplift exposes basement rocks that are significantly different from any of the other plutonic and metamorphic rocks of southern Kohistan and that are not seen elsewhere in the Pakistan Himalaya west of the Nanga Parbat-Haramosh massif (NPHM).

Rocks of the Besham area are subdivided from oldest to youngest into five groups. The oldest rocks are (1) the Besham group, metasediments and heterogeneous gneisses. In conjunction with field evidence, major, trace, and rare earth element analyses of Besham gneisses suggests that the gneisses formed *in situ* from a sedimentary protolith. The presence of both quartzofeldspathic gneiss and sodic quartzofeldspathic gneiss in the Besham group may be attributable to variable protolith composition. The Besham group was intruded by (2) mafic dikes that were subsequently metamorphosed to amphibolites. Geochemical data suggests that these tholeiitic dikes have

island arc geochemical affinities. (3) The third group of rocks compose the Lahor granitic complex, which includes cogenetic, small granitic intrusions and associated pegmatites; the Shang granite, the Dubair granite and the Shorgara pegmatite. Unconformably lying upon these three units is (4) the Karora group, which comprises conglomeratic, calcareous, and carbonaceous sedimentary rocks. The Karora group provides evidence for more than one metamorphic event in the Besham area basement uplift, *i.e.*, the Karora group is metamorphosed to middle greenschist facies, in contrast with the underlying units, which are metamorphosed to epidote-amphibolite facies. The youngest unit observed in the Besham area basement uplift is (5) a relatively undeformed leucogranite that intrudes both the Karora group and the Besham group. The leucogranite is a previously unrecognized unit.

The metamorphic and granitic rocks of the Besham area uplift may be correlative with basement exposed in the Nanga Parbat-Haramosh massif. Specifically, the quartzofeldspathic gneisses of the Besham group may correlate with the Nanga Parbat gneisses, and the amphibolites found in the Besham area may correlate with mafic dikes of the massif. Further study of both the Besham area uplift and the NPHM can provide a better understanding of Precambrian basement rocks of northern Pakistan.

Geology and Geochemistry of Indian Plate Rocks South of the Indus Suture, Besham Area, Northern Pakistan

by

James Robert LaFortune

A Thesis

submitted to

Oregon State University

in partial fulfillment of

the requirements for the

degree of

Master of Science

Completed May 20, 1988

Commencement June, 1989

Approved:

Redacted for privacy

Dr. L.W. Snee, Associate Professor of Geology in charge of major

Redacted for privacy

Dr. J.G. Johnson, Chairman of the Department of Geology

Redacted for privacy

Dean of the Graduate School

Date thesis is presented: May 20, 1988

Thesis presented by: James Robert LaFortune

ACKNOWLEDGEMENTS

I am indebted above all to one person, Kathleen Allard, for providing physical, spiritual, and monetary support for my education, not to mention a constant supply of inspired/possessed Kathie-Cookies.

Another key to my sanity at O.S.U. was Susan Ivy, office mate and friend *par excellence*, who performed cardiopulmonary resuscitation on the final draft of this manuscript. Thanks also to Dr. Larry Snee, who performed long-distance advisor duties and provided geochemistry via the U.S.G.S.

Gulzar Azeez from the University of Peshawar provided excellent field and logistical assistance in Pakistan. More important, perhaps, was his unfailing good humor and perspective on Islam and Pakistani village life. May Allah smile upon his graduate studies at Memorial University of Newfoundland. Thanks also to Shafiqur Rehman from Peshawar, who helped me navigate Pakistani bureaucracy and survive culture shock.

Dr. Robert Lawrence acquired N.S.F. grants INT 81-18403 and 86-17543, which funded this work and is gratefully acknowledged. In addition, zindabad Dr. Lawrence for his good humor when I sacrificed his 15 year old personal Brunton compass to the gods of the mighty Indus River. Thorough review of the manuscipt by Ian Madin, Joe DiPietro and John Dilles is greatly appreciated. Scott Hughes' assistance and expertise was also invaluable.

Reactor facilities and counting equipment was provided by an unsponsored research grant from the O.S.U. Radiation Center. Major element analysis was performed by XRF at the laboratories of the Denver U.S.G.S.

Lastly, I will never forget the warmth and generosity of the mountain villagers of the Besham area, who offered more chai and curious stares than I could consume in a lifetime.

TABLE OF CONTENTS

LIST OF FIGURES

LIST OF FIGURES CONTINUED

Geology and Geochemistry of Indian Plate Rocks South of the Indus Suture, Besham Area, Northern Pakistan

INTRODUCTION

The Himalaya Mountains, which stretch from Pakistan in the west to Bhutan in the east in a southward-convex arc for 2400 km across south-central Asia, are the geological manifestation of continental collision. This enormous mountain range formed largely in response to the collision of the northward-moving Indian continent with Asia beginning in the Paleocene and Eocene (Molnar and Tapponnier, 1975; Powell, 1979; Klootwijk *et al.*, 1985). Indeed, seismic, geodetic, and geologic evidence indicates that India continues to plow northward into Asia today at a rate of 4-5 mm/yr (Jacobs and Quittmeyer, 1979; Seeber *et al.*, 1981; Molnar, 1986). Thus, the rocks of the Himalaya are more than a record of the collision between India and Asia; they also contain clues to the pre- and post-collisional history.

The suture along which India collided with Asian or Cimmerian microplates (Sengor, 1979) is known as the Indus Suture Zone (ISZ). In northern Pakistan the Indus Suture bifurcates into two major faults, which surround a mainly Cretaceous-Paleogene island arc terrane, the Kohistan-Ladakh arc. The northern branch is known as the Main Karakoram thrust (MKT); the southern branch is the Main Mantle thrust (MMT). The MMT, which was first recognized as a throughgoing suture by Tahirkheli and Jan (1979), separates ultramafic and mafic oceanic rocks of the southern margin

of Kohistan from gneisses, granites, and metasediments of the northern margin of the Indian continent.

As the MKT and MMT resulted from the collision (and possible later adjustment) of India and Asia, tectonostratigraphic subdivisions of the northern margin of the Indian subcontinent in northwest Pakistan also largely reflect this collision (Fig. 1)(Yeats and Lawrence, 1984). From north to south, these subdivisions are (1) the southern Kohistan metamorphic and plutonic terrain, located adjacent to the MMT (Martin *et al.*, 1962; Calkins *et al.*, 1975; Lawrence *et al.*, 1988), (2) the Hill Ranges, where shelf sediments on the northern margin of the Indian continent were thrusted south over the Potwar Plateau along the Main Boundary thrust (MBT), which is late Tertiary (Yeats and Hussain, 1987), and (3) the Salt Range-Potwar Plateau molasse basin, where Late Cenozoic molasse is cut by active faults (Yeats *et al.*, 1984).

A newly recognized basement uplift exists in southern Kohistan, adjacent to the MMT (Fig. 2). Two significant north-trending high-angle fault zones near Besham village bound the uplift on the east and west (M.S. Baig, personal commun., 1987). The fault zone on the east is shown in Figure 2. The fault zone on the west is located 2 km west of the western margin of Figure 2.

The Besham area basement uplift exposed basement crystalline gneisses unconformable under sedimentary rocks. Both this basement and its cover are significantly different from any of the other plutonic and metamorphic rocks of southern Kohistan. They are not seen elsewhere in the Pakistan Himalaya west of the Nanga Parbat-Haramosh Massif (NPHM). They may correspond to the older basement exposed in the massif. Thus, a

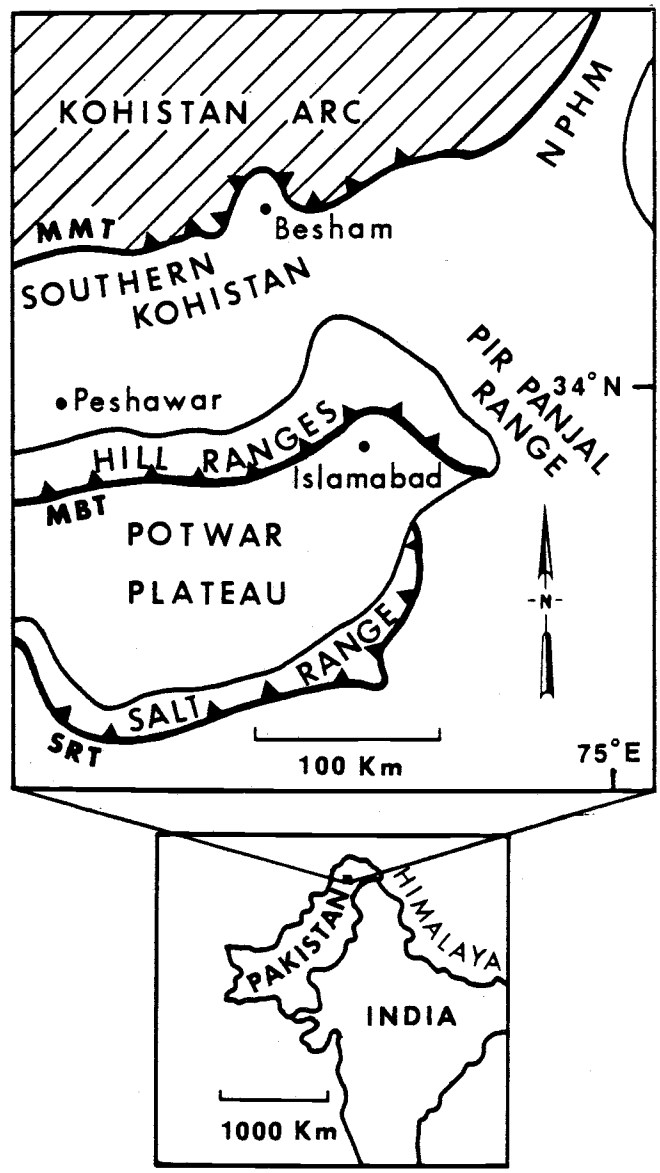

Fig. 1. Tectonic subdivisions of northern Pakistan. MMT = Main Mantle Thrust, NPHM = Nanga Parbat-Haramosh Massif, MBT = Main Boundary Thrust, SRT = Salt Range Thrust.

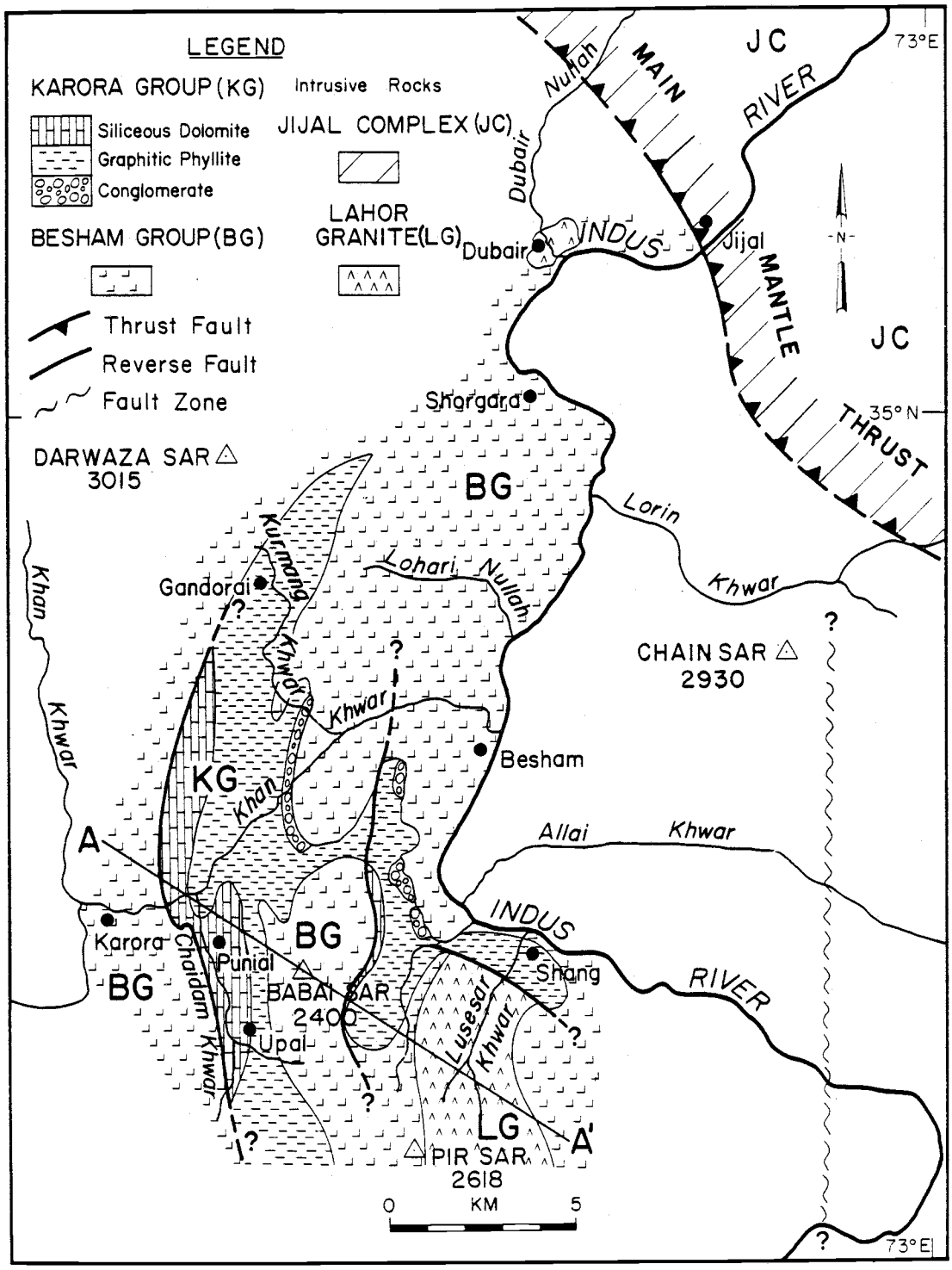

Fig. 2. Geologic map of the Besham area, northern Pakistan.

geologic study of the uplift potentially can provide a better understanding of Precambrian rocks in northern Pakistan.

The purpose of this study, therefore, is to geologically and geochemically characterize the uplifted basement block in the area near Besham village. In brief, the geology of the uplifted block consists of a polymetamorphic complex of (1) basement gneisses and metasediments (the Besham group), (2) amphibolites, (3) several small granitic intrusions and associated pegmatites (the Lahor granite), unconformably overlain by (4) conglomeratic, pelitic, and calcareous metasedimentary rocks (the Karora group). All of these units were intruded by (5) a leucogranite. In order to better constrain the geology of the Besham area, this study also presents new data for two units adjacent to the Besham area basement uplift. These units include the Mansehra granite, which intruded Indian continental crust southeast of Besham and the Swat granite gneiss, which is a highly deformed granite that intruded Indian continental crust in southern Kohistan west of Besham. These geological and geochemical data are used to shed light on the tectonic development of the Himalaya.

METHODS

Field mapping and geochemical sampling of 120 square kilometers of the Besham area was conducted in autumn, 1985. Field mapping was done on the 1:50,000 Survey of Pakistan topographic map 43-B/13 enlarged to 1:32,000. Forty-two samples were collected for microfabric and modal analysis. Nineteen samples of fresh rock weighing 4-8 kg were collected for chemical analysis. Samples for chemical analysis were crushed in a Lamaire jaw crusher and rotary mill with 99.5% pure alumina ceramic plates. A representative aliquant of each crushed sample was powdered to less than 200 mesh in a SPEC alumina ceramic shatterbox and split into two representative fractions for chemical analysis by x-ray fluroescence spectroscopy (XRF) and instrumental neutron activation analysis (INAA).

Major element analysis was done at the U.S. Geological Survey, Denver, U.S.A., by XRF using a Phillips PW1600 simultaneous wavelength-dispersive spectrometer according to the method of Taggart *et al.* (1981). Samples were incorporated in lithium tetraborate fusion discs prepared by the method of Taggart and Eahlberg (1980a, 1980b). In summary, approximately 0.8 gram of rock powder (< 100 mesh) was weighed into an ignited, tared, platinum-gold (95:5) crucible. The samples were then ignited for 20 minutes in a muffle furnace at 925° C, cooled in a desiccator, and reweighed. To the samples were added 8 grams of lithium tetraborate and the mixture was reheated to 1120° C for 17 minutes. During the reheating the mixture is in constant motion to insure homogeneity of the mixture. The resultant glass discs are analyzed on the x-ray spectrometer, which is on-line with a computer.

Trace element analysis was performed at the Oregon State University Radiation Center TRIGA reactor by INAA using the methods described by Laul (1979). Samples were irradiated in a rotating rack with an equivalent amount of the USGS standards G-2, BHVO, SRM-1633, BCR-1, and GSP-1. Irradiation was conducted for 4 hours under a neutron flux of $3X10^{12}$ neutrons per second. Samples were repackaged after irradiation and allowed to decay for seven to ten days before each gamma ray spectrum was collected for 6000 seconds on a Ge(Li) detector coupled to a 2048 channel pulse-height analyzer. After an additional 30 days, gamma-ray spectra of the samples were analyzed for 20,000 seconds. Rare earth element (REE) abundances are normalized to C1 chondrite (Anders and Ebihara, 1982).

GEOLOGIC SETTING

The geology of the Besham area was generally outlined by Ashraf *et al.*, 1980, Butt, 1983, and Fletcher *et al.*, 1986 in geological studies of larger areas within the southern Kohistan metamorphic and plutonic terrain. All of these studies were primarily concerned with the origin and association of lead-zinc deposits in this region. Informal nomenclature for rock units of the Besham area was established in these earlier works, and the present study has confirmed the usefulness of some of these names. Thus, where possible, earlier names are retained. In other cases, however, earlier nomenclature is abandoned or revised. In the geologic description that follows, discussion of the previous nomenclature is included where appropriate.

Rocks of the Besham area generally can be subdivided from oldest to youngest into five groups. The oldest rocks, which were named the Besham group by Fletcher (1986), are heterogeneous gneisses and metasediments. The second-oldest rocks are mafic dikes that intruded the Besham group and were subsequently metamorphosed to amphibolites. The third group of rocks is herein referred to as the Lahor granitic complex, which includes cogenetic, small granitic intrusions and associated pegmatites. The Shang and Dubair granites, previously named by Ashraf *et al.*, 1980, and the Shorgara pegmatite, newly named in this paper, are part of the Lahor complex. The fourth group is the Karora group, which lies unconformably upon these three units. The Karora group was first described by Jan and Tahirkheli (1968) and was named by Fletcher (1986). The Karora group comprises conglomeratic, calcareous, and carbonaceous sedimentary rocks.

The fifth unit is a leucogranite that intrudes both the Karora and Besham groups. The leucogranite is the youngest unit described in the Besham area basement uplift. Figure 2 is a geologic map that shows the distrubution of these units within the study area; Figure 3 is a stylized sketch of surface geology demonstrating cross-cutting relationships in the Besham area; Figure 4 is a cross-section through the area. Details of each of the five units are considered below.

Geology of the Besham group

The Besham group is a heterogeneous basement complex that includes quartzofeldspathic gneisses, micaceous and graphitic schists, and minor quartzites and carbonates. The group is characterized by tight, upright to recumbent isoclinal folds that plunge steeply northward. Tectonic lenses, pods, and boudins are common. Foliation in the Besham group strikes predominantly northward, and dips steeply west or east. All units in the Besham group were intruded by the Lahor granite and are unconformably overlain by the Karora group. In the study area, no units older than the Besham group have been found.

Quartzofeldspathic gneiss and sodic quartzofeldspathic gneiss represent about 50-60% of the Besham group. The sodic quartzofeldspathic gneiss was not distinguished from the quartzofeldspathic gneiss in the field. The gneisses are light-grey, medium-grained, equigranular and contain 5 to 12% biotite. Other minor and trace minerals include muscovite, epidote, magnetite, zircon, sphene, and apatite. Garnet is not present.

The texture of the gneisses varies from unfoliated to moderately gneissic, although gneissic banding is often thin and discontinuous. In thin

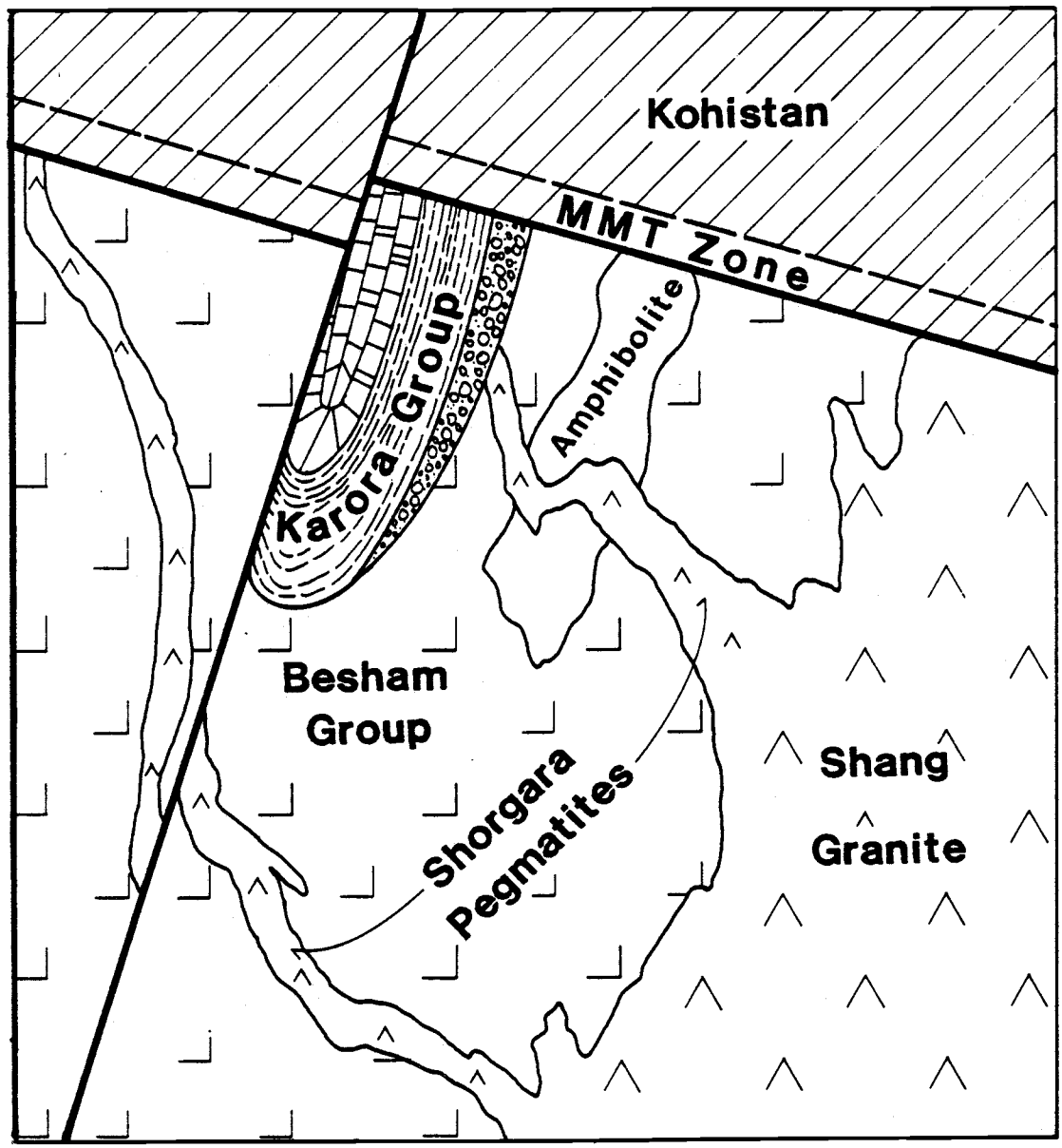

Fig. 3. Stylized sketch of surface geology demonstrating cross-cutting relationships in the Besham area. No scale is implied.

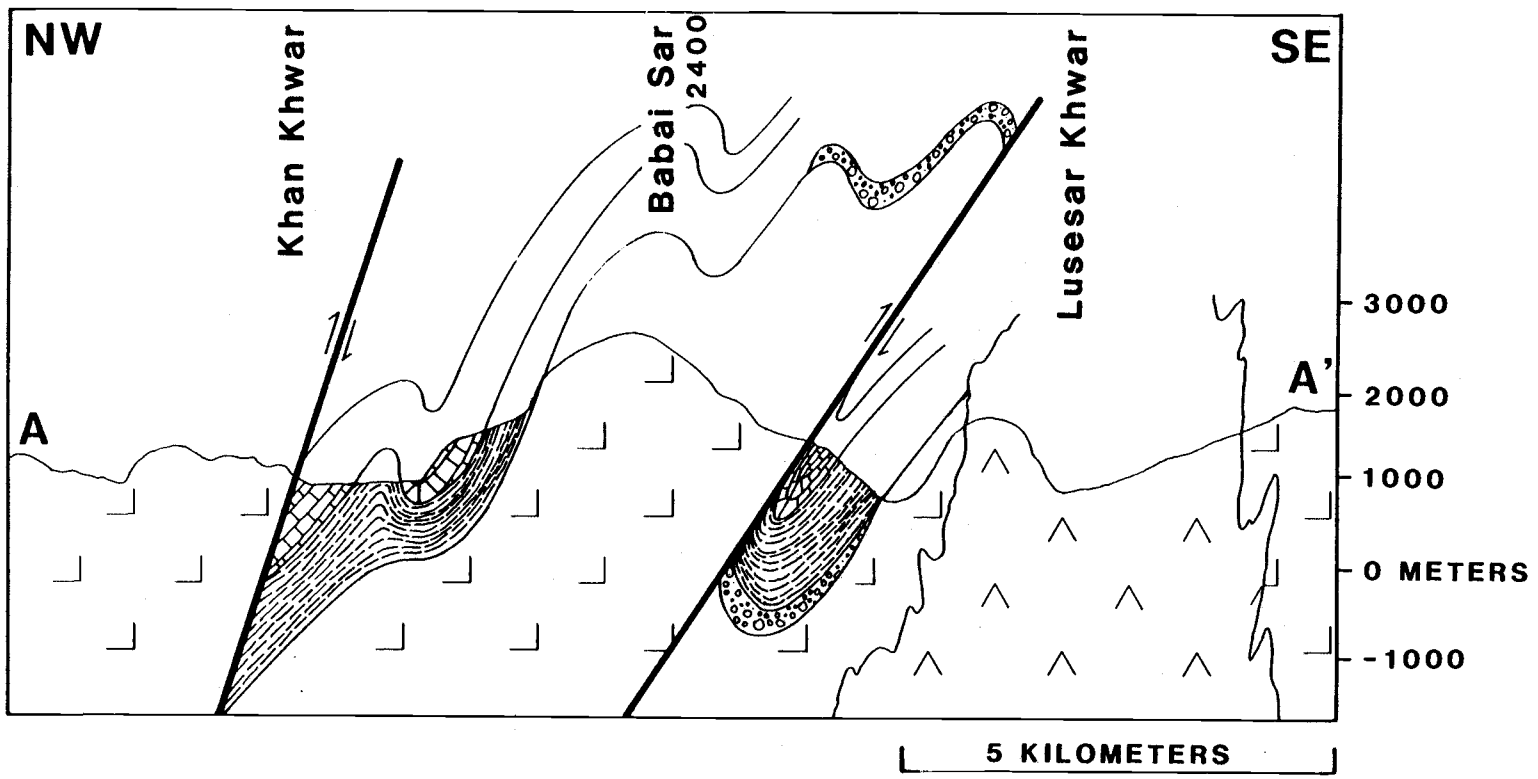

Fig. 4. Geologic cross-section of the Besham area along A-A'.
For identification of symbols, see Figure 2.

section the gneiss commonly exhibits bent albite twins and/or shear bands of finer-grained quartz within the equigranular domain, indicating tectonic reduction of grain size. The mineral assemblage of the gneisses is representative of epidote-amphibolite facies metamorphism.

Pelitic metasediments constitute the second most abundant lithology within the Besham group. These metasediments include very fine- to medium-grained graphitic schists and mica schists. The individual schist layers are heterogeneous and discontinuous and thus are not separated from the rest of the Besham group on Figure 2.

Highly sulfurous graphitic schist within the Besham group occurs as laterally discontinuous layers and pods up to 30 m thick. Contacts of the graphitic schist with the Besham gneisses are generally sharp. The mineralogy of the schist consists of very fine-grained quartz, feldspar, biotite, muscovite, and 4 to 10% graphite, with small crystals of pyrite. Abundant quartz-rich bands up to 4 cm thick are ptygmatically folded within the graphitic schist. The protolith of the graphitic schist was probably an anoxic marine silty mudstone deposited on the northern margin of the Indian plate; the quartz-rich layers in the schist were probably sandy interbeds within the clay-rich muds.

Mica schist of the Besham group commonly grades laterally into graphitic schist. The mica schist varies from fine- to medium-grained, and from a schistose to a weakly gneissic fabric. Major minerals in the mica schist include up to 90% quartz and feldspar, with lesser biotite and/or muscovite. Mineral content of the schist, however, is highly variable, and biotite may constitute up to 40% of a given specimen. Zircon, apatite, sphene, and graphite are typical accessory minerals. A trace of garnet may

be present, and garnet is commonly intergrown with biotite, suggesting that the rock reached incipient garnet-zone metamorphism. Mineralogy of the mica schist and the graphitic schist is representative of epidote-amphibolite facies metamorphism.

In addition to pelitic metasediments and quartzofeldspathic gneisses, the Besham group includes minor beds of quartzite, carbonate, and rarely, calc-silicate gneiss. The quartzites are impure and consist of quartz, feldspar, and muscovite, with traces of sphene, zircon, and rutilated biotite. Pure quartzite pods uncommonly occur as lenses of a few meters dimension within the Besham group graphitic schist and pelitic metasediments. In many locations, minor lenses of dolomitic carbonate up to 10 m thick are in sharp contact with the quartzite and pelitic metasediments of the Besham group. The dolomitic carbonates are impure; major minerals are dolomite and quartz, with minor biotite, calcite, and epidote. The siliceous dolomites are pale green, white, or tan, and the texture of the dolomite grains indicates recrystallization of the rock has occurred at temperatures above 100° C (Gregg and Sibley, 1984). Thin skarns are formed where pegmatites have intruded the carbonate (Ashraf *et al.*, 1980).

The carbonates of the Besham group are interlayered in places with banded calc-silicate gneiss which is up to 2 m thick. Along Kurmang Khwar (Fig 2) the calc-silicate gneiss consists of bands of coarse-grained actinolite up to 30 cm thick that alternate with felsic bands. The contact between the felsic bands and the darker actinolite-rich bands is marked by a 2 mm thick band of epidote. The actinolite is commonly poikiloblastic and only weakly aligned parallel to gneissic layering. Other major minerals include quartz and plagioclase, with trace amounts of biotite, sphene, and chlorite.

The protolith for the calc-silicate gneiss was probably a calcareous arenite (quartz-dolomite-feldspar-clay). Prograde metamorphism of rock of this composition would produce the observed metamorphic mineral assemblage. This mineral paragenesis is consistent with the epidote-amphibolite facies metamorphism noted throughout the Besham group. Because the mineral reaction quartz + epidote --> grossular garnet occurs at about 550° C (depending on epidote composition), the absence of grossular garnet indicates that the peak temperature during the most recent metamorphic event was probably less than 550° C and/or that the protolith lacked the chemistry needed to form garnet.

Geology of the pre-Karora group intrusions

Pre-Karora group intrusions include amphibolite, the Lahor granitic complex, and a tourmaline granite.

Amphibolite in the Besham area occurs as discontinuous lenses, layers, and pods within the Besham group. Most of the amphibolite bodies are less than 2 m wide, with rare exceptions up to 50 m wide. The amphibolite bodies are commmonly oriented parallel to the foliation of the surrounding gneisses and metasediments with contacts that are commonly sharp. Pegmatites of the Lahor granite cross cut the amphibolite, and the Karora group lies unconformably on top of the Lahor granitic complex, therefore, the amphibolite is older than both the Lahor complex and the Karora group.

Major minerals in the amphibolite include 20 to 40% andesine (An48), and 4 to 8% quartz. Epidote content varies from 1 to 5%, and trace minerals include sphene, pyrite, chlorite, zircon, and apatite. The dominant mafic

mineral is idioblastic hornblende, which constitutes 50 to 60% of the rock, and defines a strong foliation. The hornblende commonly displays a reaction rim of blue-green actinolite around a core of brown-green hornblende. These retrograde reaction rims may have occurred during the original metamorphism, or they may indicate a polymetamorphic history for the amphibolite. The mineralogy and texture of the amphibolite indicate metamorphism to epidote-amphibolite facies.

In addition to the above minerals, one amphibolite from near the MMT (#155) contains 25% diopside, 30% brown hornblende, and 35% andesine. The sample, like the other amphibolites, occurs as a discontinuous layer within the Besham group, but unlike the other amphibolites, it contains poikiloblastic clinopyroxene. Furthermore, the coarse-grained, strongly polygonal texture of sample 155 implies that it recrystallized slowly under static, near equilibrium conditions.

In addition to amphibolite, pre-Karora group intrusions include the Lahor granitic complex. The Lahor granitic complex consists of three comagmatic units, the Shang granite, the Dubair granite , and the Shorgara pegmatite. All three units are characterized by blue-grey microcline. The Shang granite, which has a mapped extent of 30 square kilometers in the study area, is the largest unit of the Lahor complex. The Shang granite continues beyond the southern boundary of the study area. The Dubair granite is a small body of about 0.5 square kilometer. The youngest unit of the Lahor complex is the Shorgara pegmatite.

Shang granite is exposed high above the Indus River on the steep mountainsides and ridge tops south of Shang village (Ashraf *et al.*, 1980). Shang granite is not found within Shang village, however, the name will be

retained in this work in order not to confuse the terminology established by Ashraf *et al.* (1980). Shang granite is a small pluton of foliated, coarse-grained biotite granite with distinctive blue-grey microcline. Shang granite clearly intrudes the Besham gneisses, and it is strongly deformed near its contacts with the gneisses. Deformation in the granite decreases away from the contacts. The blue-grey microcline crystals are up to one cm long, and aggregates of rutilated biotite crystals are common. Sphene is an abundant (3%) accessory mineral, with lesser amounts of zircon, calcite, and apatite, and trace amounts of metamorphic epidote . Broken and bent albite twins in plagioclase within the granite resulted from post-crystallization deformation.

Exposed 15 km north of Besham on the KKH near Dubair village is a small intrusion (0.5 km^2) of biotite granite with blue-grey microcline. Known as the Dubair granite (Ashraf *et al.*, 1980), the rock contains passively stoped blocks of Besham quartzofeldspathic gneiss. The Dubair granite, like the Shang granite, is strongly deformed near its contacts, and deformation decreases away from the contacts. The mineralogy of the Dubair and Shang granites are similar, except that the Dubair granite contains more mafic minerals, including 7% hornblende, and less sphene, about 1%. In addition, plagioclase in the Dubair granite is partially altered to sericite .

The Shorgara pegmatite, the youngest unit of the Lahor granitic complex, is a distinctive "blue" pegmatite with abundant blue-grey microcline. The pegmatite includes both "blue" and/or white microcline. Biotite and black tourmaline are common, though not ubiquitous, accessory minerals in the white pegmatites.

The Shorgara pegmatite intrudes all the lithologies of the Besham group. Contacts between the Shorgara pegmatite and the Besham group

rocks are sharp, except at the Besham gneisses/pegmatite contacts, where both gradational and sharp contacts are noted. Thin skarns formed where the pegmatite intruded siliceous dolomite of the Besham group. The pegmatite is best exposed near the small village of Shorgara on the KKH midway between Besham and the MMT, where there are relatively massive and abundant outcrops of this unique rock.

The pegmatites are extensively boudinaged, isoclinally folded and metamorphosed. Along the KKH between Dubair village and the MMT the pegmatites bear the same blastomylonitic overprint as the gneisses and metasediments of the Besham group (Lawrence and Ghauri, 1983). The pegmatites are truncated by the MMT, and they are truncated by the unconformity separating the Besham group from the Karora group.

The presence of abundant bluish-grey microcline in all three units of the Lahor granitic complex is considered to be evidence that they are comagmatic. Furthermore, Shorgara pegmatite cross-cuts all units of the Besham group, yet it is found only at the margins of the Shang granite. Although the three units of the Lahor granitic complex are not in immediate proximity with each other, they are all younger than the Besham group but older than the Karora group. Chemical data supporting this correlation are presented below.

In addition to the three exposed units of the Lahor granitic complex, tourmaline granite intruded within or near the study area before deposition of the Karora group. The tourmaline granite occurs only as a large (0.3 x 0.2 m) boulder within the basal conglomerate of the Karora group. The boulder is a relatively undeformed, coarse-grained granite with 5% magmatic muscovite, 3% black tourmaline, and no biotite. The source region for the tourmaline

granite boulder is not known, but it is assumed that it was not transported far. It is also important because an 40Ar/39Ar age-spectrum analysis of the magmatic muscovite is expected to yield a maximum age for the unconformity that underlies the Karora group conglomerate.

Geology of the Karora group

The name Karora group is a misnomer because rocks of the Karora group do not crop out at Karora village, however, the name will be used in this work in order not to confuse the terminology established by Fletcher (1986). The Karora group is a sequence of marine metasediments that was deposited unconformably on top of Besham group, amphibolite, and Lahor granitic complex, then synclinally folded. Foliation in the Karora group, like that of the enveloping Besham group, is primarily north trending and steeply east or west dipping. The distinctive unconformity between the Karora group and underlying Besham group, first recognized by Jan and Tahirkheli (1969), is marked by a metamorphosed pebble conglomerate that grades upward into a thick unit of graphitic phyllite, which is overlain by a jointed siliceous dolomite. Gradations between these units and wide variations within them are common.

Biotite is present in the Karora group, chlorite is sparse, and garnet is not present, therefore the Karora group is representative of middle greenschist facies. Evidence for a difference in metamorphic history across the unconformity that separates the Besham group from the Karora group is considered in the discussion section of this work.

The areal extent of the Karora group has been substantially underestimated by previous workers (*e.g.* Ashraf, 1980; Butt, 1983; Coward

et al.,1982; Fletcher *et al.*, 1986). The eastern and southern contacts of the Karora group, in particular, extend much farther than previously believed (Fig. 2). Indeed, the basal pebble metaconglomerate lies as close as 1 km to the Karakoram Highway at Chaman village, 3 km north of Shang.

The pebble metaconglomerate of the Karora group is exposed irregularly along the eastern edge of the Karora group, at the unconformity with the Besham group. The metaconglomerate is 6-10 meters thick and poorly sorted, and clasts include subrounded to angular pebbles and cobbles of the underlying basement complex. Boulders range up to 40 cm long. The conglomerate is clast-supported nearest the unconformity and for about 5 meters above the basal contact. The clast/matrix ratio diminishes as the metaconglomerate grades upwards into fine-grained graphitic phyllite.

The mineralogy of the black, pelitic matrix of the metaconglomerate consists of very fine-grained feldspar, quartz, and lithic fragments, with minor biotite and trace amounts of graphite, muscovite, sphene and detrital zircon . Most lithic fragments are poorly sorted and angular, although they commonly lie parallel to the weak foliation of the matrix. The matrix contains quartz-rich and mica-rich segregation bands that define foliation; detrital zircon and sphene tend to concentrate within the mica-rich bands. The relative proportion of mica and graphite to quartz and feldspar increases rapidly and gradationally upwards into overlying graphitic phyllite.

The metaconglomerate is deformed. The amount of deformation of pebbles within a single outcrop varies according to competency of pebble lithology. Pebbles of competent rock such as tourmaline granite lack the flattening and folding seen in the less competent carbonate and graphitic clasts.

Discontinuous beds of intraformational, matrix-supported pebble metaconglomerate are common within the massive graphitic phyllite, however, they are inseparable from the graphitic phyllite at the scale of this study. The principal differences between the intraformational and the basal metaconglomerates are (1) the intraformational beds are not clast-supported, and (2) pebbles are mostly graphitic schist, quartzite, and carbonate, and lack the granitic clasts common to the basal unit.

Massive, fine-grained graphitic phyllite is the most extensive unit of the Karora group, and is relatively easily recognized throughout the field area. The Karora group graphitic phyllite is more extensive in outcrop than the lithologically similar graphitic schist of the Besham group. Excellent exposures of massive, poorly indurated, black graphitic phyllite crop out in roadcuts along the Besham-Karora road. The rock invariably contains abundant, discontinuous, ptygmatically folded quartzose veinlets up to 3 cm wide and 10 cm long. Crenulation cleavage is common.

The mineralogy of the graphitic phyllite consists of dusty, submicroscopic graphite, quartz ribbons with ragged, sutured quartz-quartz grain boundaries, fine-grained plagioclase, biotite, muscovite, minor epidote and chlorite, and trace amounts of detrital zircon. The epidote occurs as amorphous masses within quartz- and plagioclase-rich domains.

The Karora group graphitic phyllite commonly grades into extremely fine-grained, black, dirty quartzite and/or metapelite. The best exposures of these two lithologies occur along the Kurmang Khwar on the road near Gandorai (Fig. 2). Major minerals in the dirty quartzite include very fine-grained quartz, feldspar, biotite, and anhedral muscovite blades, with trace amounts of graphite, zircon, and tourmaline. The extremely fine grain size

(< 0.1 mm) of the dirty black quartzite gives the rock a homogeneous bluish-black appearance, and there is a weak, slaty parting parallel to foliation. Thin folia and quartz veinlets are less than 1 mm apart, and on some surfaces a slight phyllitic sheen is evident.

Graphitic phyllite locally grades into metapelites, ranging from medium-grained psammitic biotite schist to extremely fine-grained muscovite-biotite metapelite. The metapelites occur in discontinuous beds less than 20 m thick. The muscovite-biotite metapelite typically weathers to a light brown-orange color, and is locally aphanitic. Quartz, feldspar, and micas compose the major minerals, with traces of zircon, graphite, and sphene.

The metapelites and graphitic phyllite are in sharp, conformable contact with the Karora group carbonates. The carbonate is exposed in an elongate north-trending unit that reaches its maximum thickness of about 500 meters between Upal and Punial villages. It pinches out laterally to the south of Upal and to the north of the Besham-Karora road.

The most abundant carbonate is a dark grey to black siliceous metadolomite that is well exposed along the Besham-Karora road. The rock has quartzose interlayers in vein-like segregations up to 4 cm thick. Mineralogy of the siliceous metadolomite consists of 70% fine-grained (< 0.2 mm) dolomite and 30% strained, subangular quartz with a trace of muscovite. Both dolomite-dolomite and quartz-quartz grain boundaries are sutured and irregular. The nonrhombic, mosaic texture of the dolomite crystals is typical of xenotopic-A (anhedral) dolomite, which is thought to result from either recrystallization of a preexisting dolomite at temperatures above 100°C, or from replacement of a limestone by dolomite (Gregg and

Sibley, 1984). Both Karora group and Besham group dolomites clearly display this recrystallized texture.

There are many lithologic variations within this relatively extensive carbonate sequence. For example, the 40-m-wide carbonate outcrop west of the mouth of Chaidam Khwar on the Besham-Karora road is made up of two distinctive lithologies. The outcrop nearest Chaidam Khwar is a tan-buff colored sandy dolomite that powders easily to a yellowish grit. Farther from the stream is a more crystalline, white siliceous dolomite with two pervasive pressure solution cleavage planes spaced 2 cm apart that cause the rock to break readily into elongate, rectangular prisms.

Other variations within the carbonates of the Karora group include etched grey-blue limestone that commonly crops out as discontinuous beds within the massive graphitic phyllite. Also, a 100 m long by 10 m thick outcrop of limestone breccia was found at 1785 m elevation on the steep ridge northeast of Punial village. Clasts in the breccia are angular grey-blue limestone up to 5 cm long, and subangular dissolution pits are prominent where the clasts have dissolved/eroded more rapidly than the limey sand matrix, commonly leaving fragile, reddish-brown skeletal clasts in the pits. The breccia indicates that instability and slumping occurred within the Karora group carbonate.

Geology of a post-Karora group intrusion

Near the western contact of the Karora group with the Besham group along the Besham-Karora road the graphitic phyllite of the Karora group is intruded by several small sills of equigranular, medium-grained leucogranite of color index 2 to 7 (Fig. 2). Small sills of the leucogranite also intrude the

Besham group west of the mouth of Chaidam Khwar. The leucogranite is important because it is the only post-Karora group unit recognized within the Besham area basement block, and because it is clearly younger than the Karora group, which was previously considered to be the youngest unit within the basement block (Ashraf *et al.*, 1980; Butt, 1983; Coward *et al.*, 1982; Fletcher *et al.*, 1986).

The leucogranite is faint red on fresh surfaces and weathers white. Its best exposure is located east of the mouth of Chaidam Khwar, where the largest sill is 25 m thick. Karora group graphitic phyllite within a few meters of the contact is baked to an extremely hard, dense, coarse-grained graphitic schist. Mineralogy of the leucogranite consists of oligoclase that is altered to sericite (with optically continuous unaltered oligiclase overgrowths), quartz , microcline, biotite, and accessory pyrite and sphene. Quartz-quartz grain boundaries are sutured to weakly polygonal. Plagioclase is occasionally myrmekitic. Biotite defines a very weak foliation in the leucogranite, which provides evidence for at least minor deformation after metamorphism of the Karora group and emplacement of the leucogranite.

Geology of units adjacent to the Besham area

The geology of two units of regional significance will be briefly discussed below in order to better constrain the geology of the Besham area. The two units are the Mansehra granite and the Swat granite gneiss.

Late Precambrian-Cambrian Mansehra granite intrudes metasedimentary rocks of possible Precambrian age southeast of Besham (Ashraf *et al.*, 1980; LeFort *et al.*, 1980). This porphyritic granite is truncated against a major north-trending fault zone that separates the Besham area

basement complex from the Mansehra pluton and associated metasediments (M.S. Baig, personal comm., 1987). The fault zone, therefore, is younger than the Mansehra granite. The fault zone is located on the east side of the Indus River (Fig. 2). Mansehra granite is a peraluminous, cordierite-bearing pluton, dated by LeFort *et al.* (1980) at 516 ± 16 m.y. An analysis of major element and rare earth element (REE) data from the Mansehra granite will be presented in the geochemistry section.

The Swat granite gneiss is a suite of porphyritic granites that is similar to the Mansehra granite and is exposed in the lower Swat region, west of Besham (Martin *et al.*, 1962; King, 1964). The age of the Swat granite gneiss is not known, but it is thought to be similar to the age of the Mansehra granite (Lawrence *et al.*, 1988). The oldest unit of the Swat granite gneiss, the Choga granite, crops out 10 km west of Karora (Martin *et al.*, 1962; J. DiPietro, personal commun., 1987), west of the fault zone that bounds the Besham area basement block. The Choga granite is a porphyritic biotite garnet granite with a moderate to strong gneissic texture. An analysis of geochemical data from the Choga granite will be presented in the geochemistry section.

Structure of the Besham area basement uplift

The Besham area basement uplift is bound on the east and west by high angle, north-trending fault zones (Fig. 2)(M.S. Baig, personal commun., 1987). Structures found within the Besham group include tight, upright to recumbent isoclinal folds with an amplitude of 1-3 meters. These small structures are syn- or post-tectonic due to the extreme transposition of layering that created the discontinuous tectonic lenses, pods, and boudins

found throughout the Besham group. In addition, major north-trending, tight, upright folds with a wavelength of 1-2 km affect all the units of the Besham area basement uplift (Fig. 4). The Karora group was deposited unconformably on top of the Besham group, then enveloped and preserved within synclines formed by these folds. Within the field area, the western limbs of these synclines are cut by high angle north-trending reverse faults that juxtapose the Besham group and the Karora group (Figs. 2 and 4). In the cross-section (Fig. 4) the basal conglomerate has been shown in its uplifted position to illustrate the offset on one of these faults, however the geologic map pattern (Fig. 2) makes it clear that the conglomerate is only locally present in this position.

The Besham group, Lahor granitic complex, and Karora group exhibit a predominantly north-trending foliation that dips steeply to the east or west. The exception to this dominant foliation occurs adjacent to the MMT, where Indian plate rocks are overprinted by a strong blastomylonitic fabric that is parallel to the orientation of the MMT (Lawrence and Ghauri, 1983). The leucogranite has a very weak foliation defined by biotite, and is the least foliated of the units within the Besham area basement uplift.

GEOCHEMISTRY

Nineteen samples from the Besham area were analyzed for major and selected trace elements. Sample locations are shown on Figure 5. The samples included five gneisses of the Besham group, four amphibolites, five plutonic rocks of the Lahor granitic complex, the tourmaline granite boulder and the post-Karora group leucogranite. In addition, one sample of the adjacent Mansehra granite and two samples of the Swat granite gneiss were analyzed. Geochemical data are presented in Table 1. Major element concentrations are given in weight percent (wt. %), trace element concentrations in parts per million (ppm). In the context of this paper, the term major element is used for chemical constituents whose abundance in common rocks is normally greater than 0.1 wt. %; trace element is used for an element whose abundance in common rocks is less than 0.1 wt. %.

Major elements

The Besham group gneisses include sodic quartzofeldspathic gneiss and quartzofeldspathic gneiss. Both types of gneisses are equigranular, peraluminous, calcium-poor (< 1.5 wt. % CaO) and corundum normative. An A-C-F diagram clearly demonstrates their bimodal nature (Fig. 6)(Ca=CaO, K=K_2O, Na=Na_2O). On a ternary Q-A-P diagram of normative quartz-alkali feldspar-plagioclase feldspar the bimodal nature of the gneisses is also evident, *i.e.*; the sodic quartzofeldspathic gneiss contains only 5% normative potassium feldspar, whereas the quartzofeldspathic gneiss contains 34% (Fig.7).

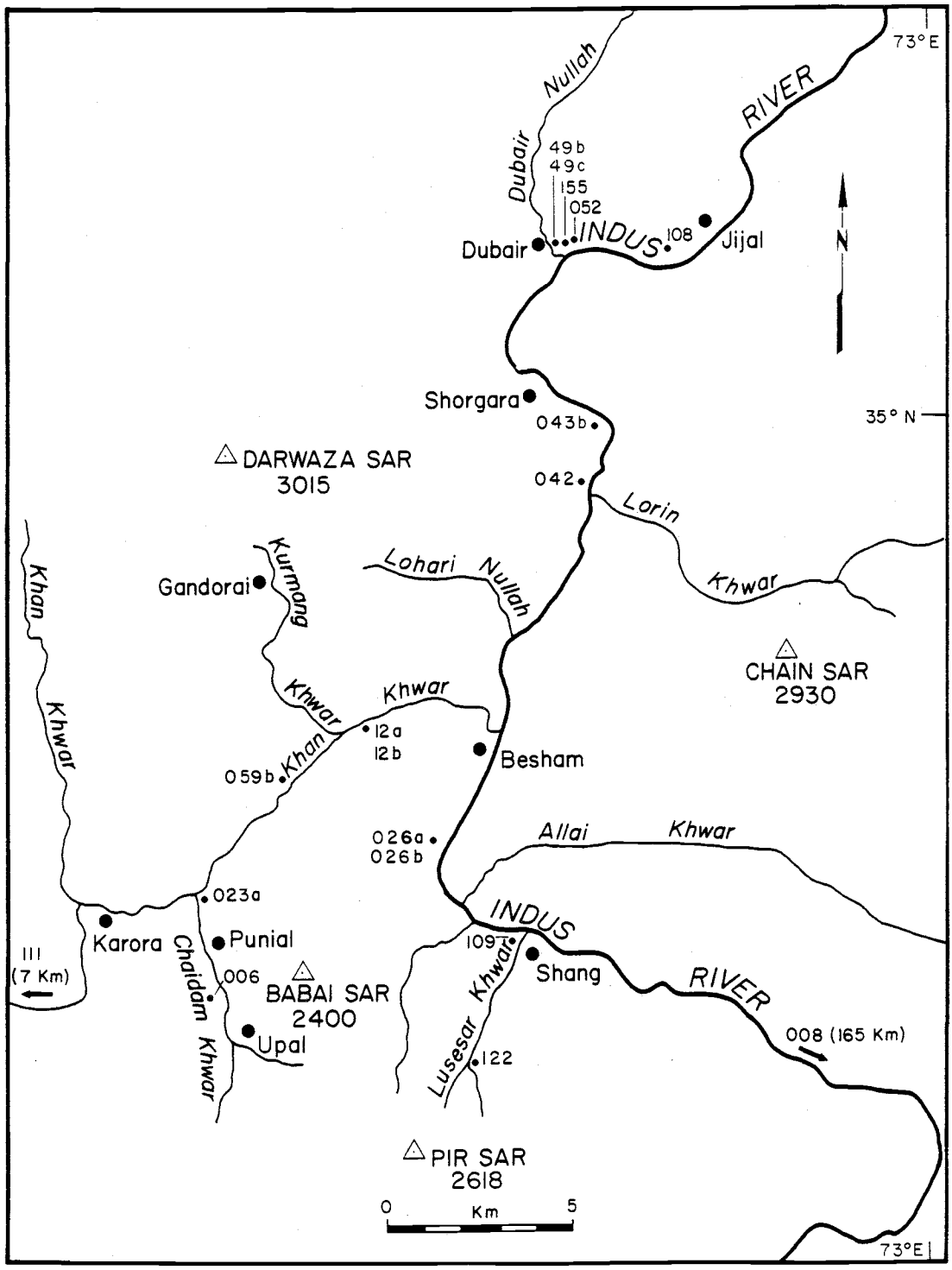

Fig. 5. Sample location map.

Table 1: Geochemistry of Representative Samples from the Besham area, northern Pakistan

Rock type:	{----------Besham sodic gneiss---------}			{--Besham gneiss--}			{-------Besham amphibolite-------}	
SAMPLE	**052**	**43b**	**26a**	**108**	**49b**	**042**	**12b**	**006**
SiO_2 (wt. %)	74.4	75.8	72.7	73.6	71.7	50.8	49.5	51.8
Al_2O_3	12.3	12.8	15.7	13.5	14.5	13.4	13.8	15.3
FeO	2.20	0.91	0.44	0.68	0.70	8.63	8.04	6.78
Fe_2O_3	1.83	0.70	0.39	0.56	0.70	3.61	3.48	3.47
MgO	0.16	0.45	0.28	0.22	0.25	6.74	7.17	6.38
CaO	0.52	0.80	1.47	1.28	1.54	10.2	10.7	9.83
Na_2O	6.12	5.34	6.86	2.90	3.32	2.80	2.62	3.60
K_2O	0.89	0.78	0.83	5.48	5.52	0.68	1.19	0.56
TiO_2	0.25	0.29	0.13	0.18	0.18	1.08	0.89	0.59
P_2O_5	<0.05	<0.05	0.05	<0.05	<0.05	0.10	0.09	0.1
MnO	<0.02	<0.02	<0.02	<0.02	<0.02	0.22	0.20	0.19
La (ppm)	70.6	41.8	16.5	56.4	37.9	6.98	7.07	11.2
Ce	162	115	25.0	123	60.5	15.2	14.2	20.0
Nd	42.6	36.2	6.8	35	17.1	-	16.0	-
Sm	11.8	10.7	1.14	7.16	2.41	3.02	2.62	2.65
Eu	1.94	1.63	0.48	0.55	0.83	1.14	0.90	0.79
Tb	1.8	1.5	0.17	0.79	0.25	0.60	0.51	0.46
Yb	5.4	5.0	0.8	2.0	1.2	2.6	2.4	1.8
Lu	0.85	0.77	0.09	-	0.15	0.47	0.32	0.22
Sc (ppm)	2.39	7.84	1.32	2.58	2.12	47.2	45.4	37.1
Cr	2.8	3.5	1.8	2.5	1.8	99	188	79
Co	1.4	0.8	1.2	0.9	1.2	52.1	51	31
Zn	9	20	10	18	18	150	140	130
Rb	40.3	19.8	16.7	303	163	21.3	33.8	21.3
Sr	40	-	450	90	470	260	200	400
Cs	1.2	0.8	0.5	3.4	1.7	-	0.9	-
Ba	157	-	195	563	1350	-	558	-
Zr	320	330	110	170	170	190	140	120
Hf	9.8	9.9	3.0	5.3	4.6	2.2	1.5	2.0
Ta	0.35	1.4	0.34	0.55	0.45	0.35	0.17	0.34
Th	1.7	7.0	4.4	55.	7.5	2.2	2.7	2.6
U	3.2	3.4	2.3	7.0	-	-	-	-

Table 1 (continued)

Rock type: {amphibolite}	{---Shang granite---}		{Shorgara pegmatites}		{leucogranite}	{tour. granite}	{Dubair granite}
SAMPLE 155	**122**	**109**	**12a**	**26b**	**23a**	**59b**	**49c**
SiO_2 (wt. %) 48.3	70.2	69.6	74.0	72.7	71.5	73.7	66.0
Al_2O_3 14.2	13.0	12.9	14.7	14.7	14.3	14.5	13.2
FeO 11.61	2.16	2.41	0.17	0.04	0.92	0.37	3.57
Fe_2O_3 3.66	1.99	4.62	0.15	0.04	0.85	0.35	2.92
MgO 7.46	0.56	0.40	0.16	0.16	0.47	0.14	0.68
CaO 12.9	1.70	2.07	1.20	0.58	1.39	0.53	3.14
Na_2O 2.64	2.92	2.80	4.86	3.37	3.78	4.34	2.86
K_2O 0.56	5.25	5.27	3.18	6.30	4.36	3.88	4.50
TiO_2 0.94	0.60	0.66	0.04	<0.02	0.30	0.03	1.09
P_2O_5 0.08	0.13	0.14	<0.05	<0.05	0.05	0.37	0.30
MnO 0.19	0.03	0.04	<0.02	<0.02	<0.02	<0.02	0.07
La (ppm) 3.95	361	261	7.07	1.81	2.49	11.1	103
Ce 8.67	712	539	11.7	1.50	39.1	19.2	201
Nd -	120	96	-	-	-	8.9	72
Sm 2.16	28.9	24.5	0.49	0.18	2.22	2.06	13.5
Eu 0.85	1.29	1.25	0.60	0.64	0.41	0.30	1.89
Tb 0.44	3.0	2.8	0.04	0.02	0.23	0.29	1.7
Yb 2.4	8.5	8.7	-	-	1.3	1.0	4.8
Lu -	0.89	0.90	0.04	-	0.08	0.10	0.76
Sc (ppm) 37.1	6.07	0.61	0.15	0.15	2.28	6.84	11.2
Cr 122	5.7	5.8	1.8	1.3	3.2	2.9	5.1
Co 53.4	3.7	3.3	0.2	0.1	2.4	0.4	6.2
Zn 120	50	60	4	2	20	30	80
Rb 19.1	282	316	64.4	151	123	153	178
Sr 140	-	180	250	340	460	63	229
Cs 0.5	5.0	7.1	0.8	1.0	3.3	7.1	3.1
Ba -	827	-	1710	6140	766	350	1370
Zr -	570	650	94	41	176	77	540
Hf 1.5	16	18	3.0	0.3	4.6	1.0	15
Ta 0.30	2.2	2.3	0.03	0.05	1.5	5.0	2.0
Th -	91.3	94.9	1.8	0.2	12.2	0.7	20.6
U -	9.5	9.4	-	-	4.4	1.0	4.9

TABLE 1 (continued)

Rock type:{Mansehra gr.}{Choga/Swat granite gneiss}

SAMPLE	008	111	004	percent uncertainty at 1 σ
SiO_2 (wt. %)	69.7	69.1	70.0	.08
Al_2O_3	15.1	14.0	13.6	.12
FeO	2.84	3.18	2.62	.01
Fe_2O_3	1.38	2.12	1.84	.11
MgO	0.93	1.83	1.49	.56
CaO	1.36	2.17	2.01	.15
Na_2O	2.78	2.24	2.41	.93
K_2O	4.88	3.11	3.38	.23
TiO_2	0.47	0.97	0.80	1.1
P_2O_5	0.21	0.06	0.1	1.7
MnO	0.05	0.1	0.06	5.5
La (ppm)	30.3	63.3	-	3
Ce	76	127	-	7
Nd	29	42	-	12
Sm	6.65	9.94	-	5
Eu	0.92	1.59	-	5
Tb	0.83	1.1	-	5
Yb	3.0	4.3	-	5
Lu	0.30	0.58	-	5
Sc (ppm)	7.70	15.0	-	3
Cr	23.2	53.2	-	10
Co	5.4	12.	-	5
Zn	45	68	-	15
Rb	297	142	-	10
Sr	-	120	-	10
Cs	25	3.8	-	5
Ba	405	799	-	12
Zr	190	340	-	15
Hf	470	9.2	-	5
Ta	2.1	1.3	-	5
Th	19.6	27.6	-	5
U	3.0	2.8	-	7

For major elements, analytical precision is based on replicate countsof in-house basalt standard BB-1 reported by USGS Denver XRF facility.
For trace and REE, anaytical precision is based on replicate counts of multiple in-house standards reported by OSU Radiation Center.

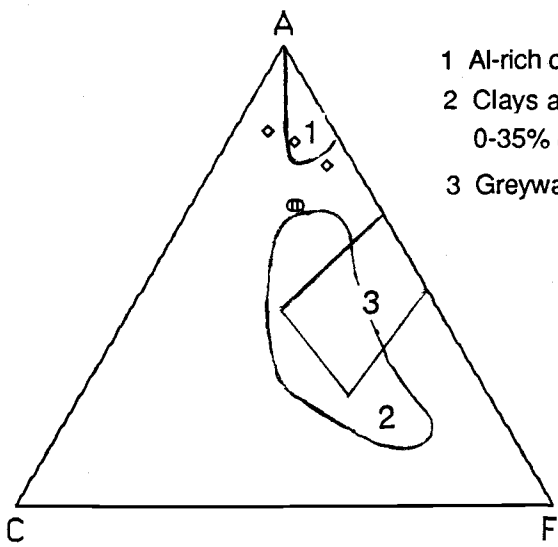

Fig. 6. A-C-F ternary diagram delineating protolith fields for Besham area samples. Plot after Nockolds, 1954.

◇ sodic quartzofeldspathic gneiss
○ quartzofeldspathic gneiss

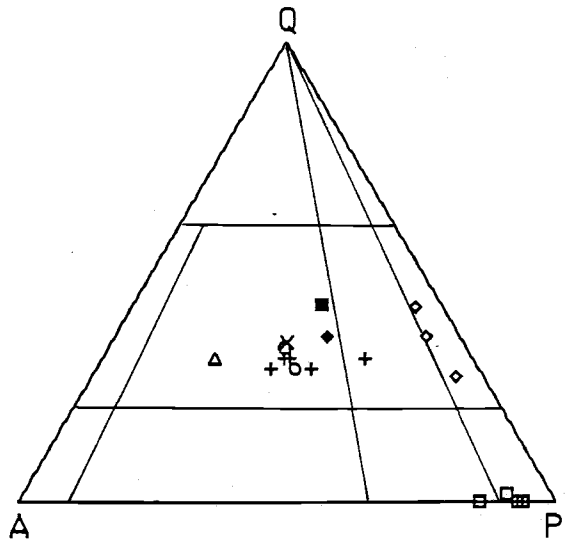

Fig. 7. Normative Q-A-P diagram of Besham area samples. Base diagram after Streckeisen, 1976.

- ◇ sodic quartzofeldspathic gneiss
- ○ quartzofeldspathic gneiss
- \+ Lahor granitic complex
- □ amphibolite
- ▲ leucogranite
- ✖ Mansehra granite
- ◆ Choga granite
- ■ tourmaline granite boulder

Figure 8 shows an A-F-M diagram of major element compositions of five Besham gneisses, in addition to twelve other samples from the Besham area ($A=Na_2O + K_2O$, $F=FeO^*$, and $M=MgO$). The $FeO^*/Na_2O + K_2O$ ratio of the sodic quartzofeldspathic gneiss exhibits a wide range of values, whereas the quartzofeldspathic gneiss values are more consistent. Mg content is relatively constant for both types of gneiss.

Spider diagrams of the Besham gneisses exhibit depletion of TiO_2 relative to average Archean upper crust in both the sodic quartzofeldspathic gneiss and the quartzofeldspathic gneiss (Figs. 9 and 10). All values presented in spider diagrams in this study are chondrite normalized (after Thompson, 1982) except rubidium, potassium, and phosphorus, which are normalized to primative mantle values after Sun, (1980). TiO_2 ranges from .13 to .25 wt. % in the sodic quartzofeldspathic gneiss, and is .18 wt % in the quartzofeldspathic gneiss. A negative trough is also seen for P_2O_5

The scatter seen in the major element data, particularly in sodium and potassium, for the Besham gneisses may be due to variability in the composition of the sediments that comprised the protolith of the gneisses. This compositional variability relative to protolith is observed in the A-C-F diagram (Fig. 6): the quartzofeldspathic gneiss plots near the field of rocks with a protolith of clays and shales containing 0-35% carbonate, and the sodic quartzofeldspathic gneiss plots within or near the field of aluminum-rich clays and shales.

Amphibolite bodies found within the Besham area basement uplift are classified as tholeiitic based on their major element content, as shown by the A-F-M diagram (Fig. 8)(Irvine and Baragar, 1971). The four amphibolite samples plot within the tholeiite field, near the calcalkaline/tholeiite

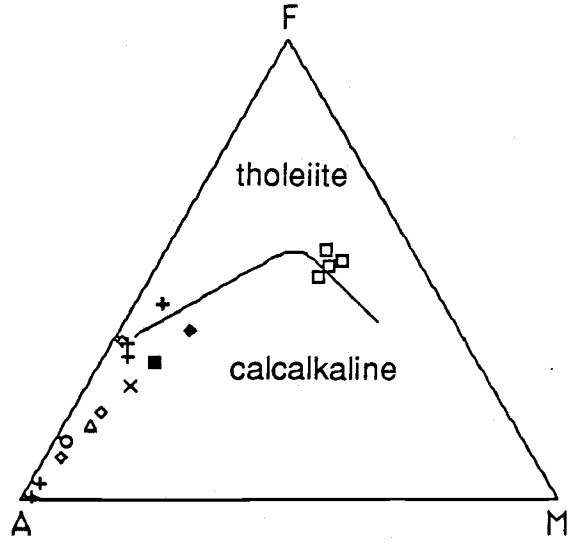

Fig. 8. A-F-M diagram of Besham area samples.
Discrimination line from Irvine and Baragar, 1978.

- ◇ sodic quartzofeldspathic gneiss
- ○ quartzofeldspathic gneiss
- + Lahor granitic complex
- □ amphibolite
- ▲ leucogranite
- × Mansehra granite
- ◆ Choga granite
- ■ tourmaline granite boulder

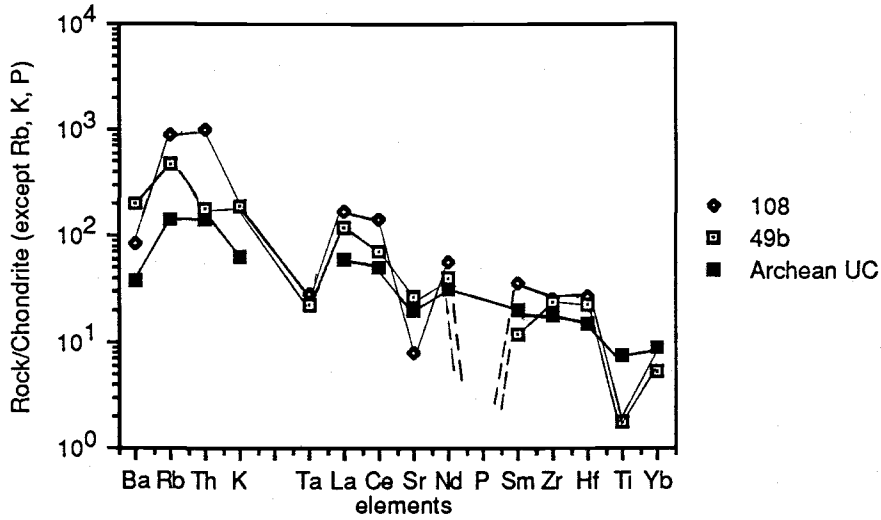

Fig. 9. Spidergrams for quartzofeldspathic gneiss. Archean upper crust from Taylor and McClennan, 1985.

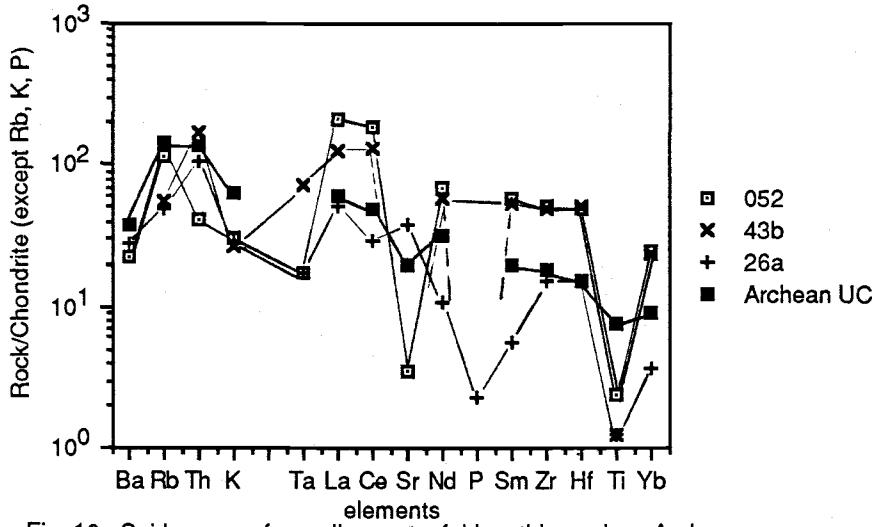

Fig. 10. Spidergrams for sodic quartzofeldspathic gneiss. Archean upper crust from Taylor and McClennan, 1985.

discrimination line. Other diagrams that distinguish tholeiitic from calcalkaline magmas (SiO_2 *vs.* FeO* and SiO_2 *vs.* FeO*/MgO; Miyashiro, 1974) suggest a tholeiitic protolith for the amphibolite (Figs. 11 and 12)

A spider diagram of the amphibolites shows a negative trough for P_2O_5 relative to the international standard basalt BHVO-1 (Fig. 13). Phosphorous content varies from .06 to 0.1 wt %. Titanium is also depleted relative to BHVO-1, although TiO_2 does not plot as a trough on the spider diagram. Potassium, a volatile-lithophile element, is depleted relative to BHVO-1, perhaps due to its mobility during metamorphism.

Figure 14 is a tectonic discrimination diagram (after Bhatia, 1983) which suggests that the amphibolite protolith was derived from an oceanic island arc setting. The diagram also demonstrates that silica (48 to 52 wt. %) and alumina (13.4 to 15.3 wt.%) content in the amphibolites have a narrow range of concentrations, as does magnesium (6.4 to 7.5 wt. %).

The Lahor granitic complex includes Shang granite, Dubair granite, and Shorgara pegmatite. Major element oxides of calcium, potassium, and sodium of the Lahor granitic complex are plotted on a ternary diagram in Figure 15. Sodium content is nearly constant for both the Shang and the Dubair granite, however, CaO varies from 3.1 for the Dubair granite to 1.7 for Shang granite sample #122. The ratio K_2O/Na_2O for the pegmatite is inconsistent, varying from 0.65 to 1.9 wt. %. All three units of the Lahor complex are moderately high in Al_2O_3, with values ranging from 12.9 to 15 wt. %, but none contain normative corundum.

On a Q-A-P ternary plot the Shang and Dubair granites cluster tightly with the Besham quartzofeldspathic gneiss (Fig. 7). The Lahor complex

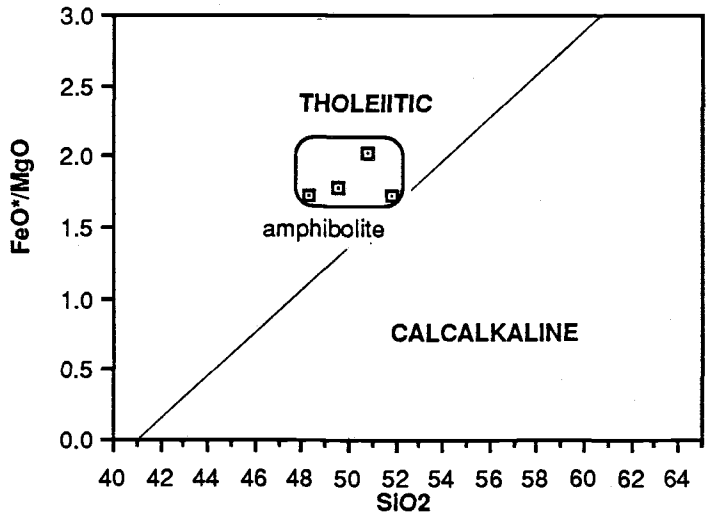

Fig. 11. SiO2 vs. FeO*/MgO diagram for mafic rocks of the Besham area. Thol./Calkalk. determination line from Miyashiro, 1974.

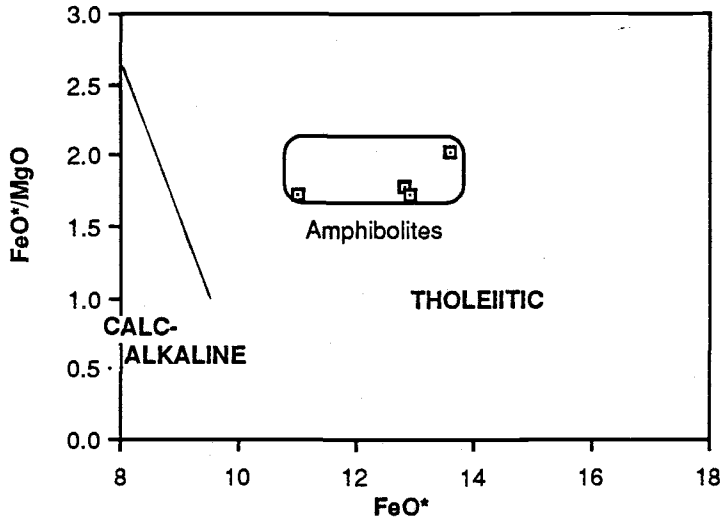

Fig. 12. FeO* vs. FeO/ MgO diagram for mafic rocks of the Besham area; after Miyashiro, 1974.

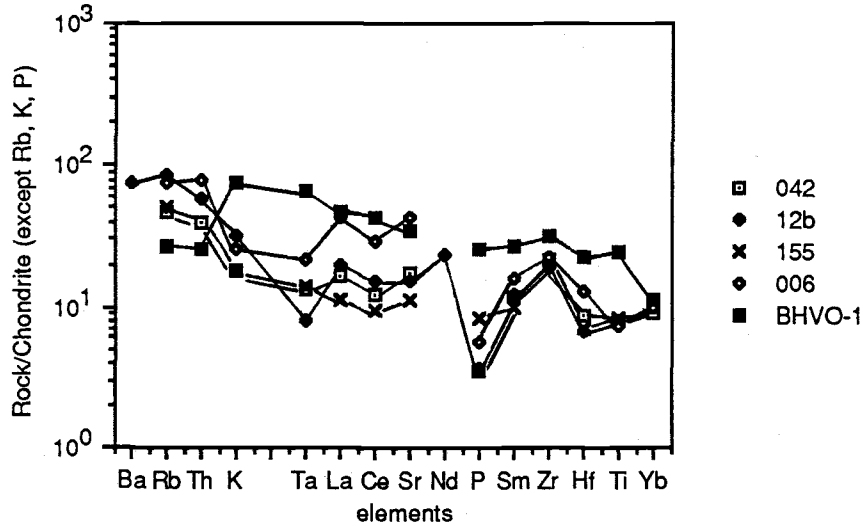

Fig. 13. Spidergrams for amphibolites. BHVO-1 from Taylor and McClennan, 1985.

datum that plots outside this cluster is the more sodic-rich pegmatite noted above.

On the A-F-M diagram the Dubair granite has greater total iron content than the Shang granite by a factor of 1.5. Magnesium content is similar for both units. Shorgara pegmatite data plot near the alkali apex, an indication of their extremely fractionated, felsic mineralogy.

A spider diagram normalized to chondrite exhibits depletion of TiO_2, P_2O_5, and K_2O in both the Shang and the Dubair granite (Fig. 16). Average Archean upper crust is also shown for comparison. TiO_2 content for Shang granite is similar to that of average Archean upper crust. The spidergrams for the Shang and Dubair granite resemble other "S-type" granites noted by Thompson *et al.*, (1984).

On a Fe_2O_3 + MgO *vs.* Al_2O_3/SiO_2 tectonic discrimination diagram (Bhatia, 1983) the Dubair granite plots within the "active continental margin" field, and Shang granite plots near the field (Fig. 14). This diagram also illustrates the iron and magnesium enrichment of the Shang and Dubair granites relative to the Besham gneisses.

On a Q-A-P diagram the tourmaline granite boulder does not plot in a cluster with the Lahor complex or Besham group rocks (Fig. 7). The tourmaline granite is more siliceous and slightly less alkalic than the other granites and granite gneisses of the Besham area. This distinction can also be seen on the A-F-M diagram. The tourmaline granite is peraluminous.

The Mansehra granite and the Choga granite are included on Figure 7. Both are peraluminous granites located adjacent to the Besham area uplift that help constrain the age and tectonic history of the uplift. The Q-A-P diagram discriminates well between the cluster of normative granite and

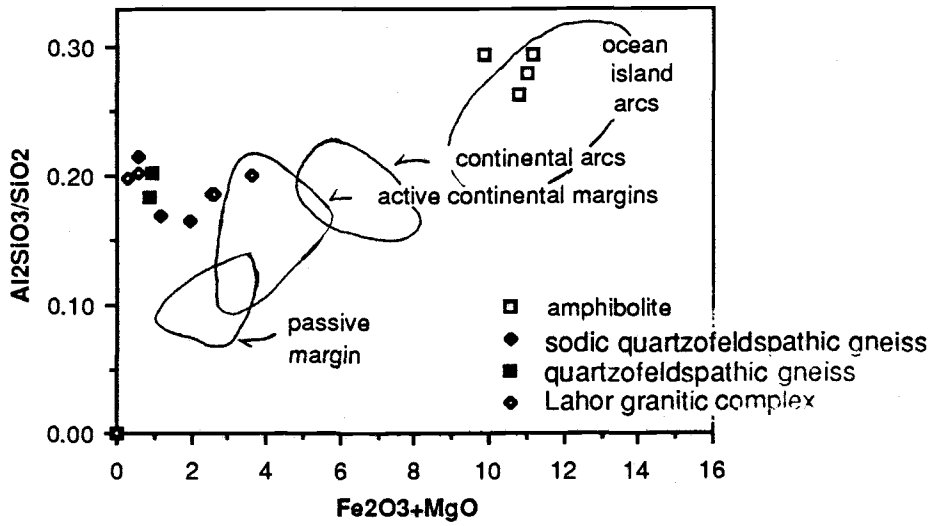

Fig. 14. Tectonic discrimination diagram of Besham area samples.
After Bhatia, 1983.

gneiss compositions located within the Besham area uplift and the Choga granite, located adjacent to the uplift. The Choga granite is also enriched in iron and magnesium relative to the Mansehra granite and the Besham area rocks. The sample of Mansehra granite has similar Q-A-P normative weight percentages to Besham quartzofeldspathic gneiss #108.

Trace elements

The concentrations of Rb, Cs, Ba, Sr, Cr, Co, Sc, Zn, Zr, Hf, Ta, Th, U, and the rare earth elements (REEs) La, Ce, Nd, Sm, Eu, Tb, Yb, and Lu are presented in Table 1. The chondrite normalized incompatible element patterns of representative samples from the Besham area are presented on both spider diagrams and REE diagrams.

Trace elements in the Besham group The K-group incompatible elements include Rb, Cs, Ba, and Sr. These elements are large cations that generally correlate positively to K_2O concentration. Figures 9 and 10 are spider diagrams that demonstrate this correlation for the quartzofeldspathic gneiss and sodic quartzofeldspathic gneiss respectively. The quartzofeldspathic gneisses contain 163 and 303 ppm rubidium, and the sodic quartzofeldspathic gneisses contain 17 to 40 ppm.

Average cesium concentration in the quartzofeldspathic gneiss is higher than in the sodic quartzofeldspathic gneiss by a factor of two. Likewise, barium is more enriched in the quartzofeldspathic gneiss relative to the sodic quartzofeldspathic gneiss by a factor of 5. Strontium in the Besham gneisses is less systematic, with quartzofeldspathic gneiss concentrations of 90 and 470 ppm, and sodic quartzofeldspathic gneiss values ranging from 40 to 450 ppm.

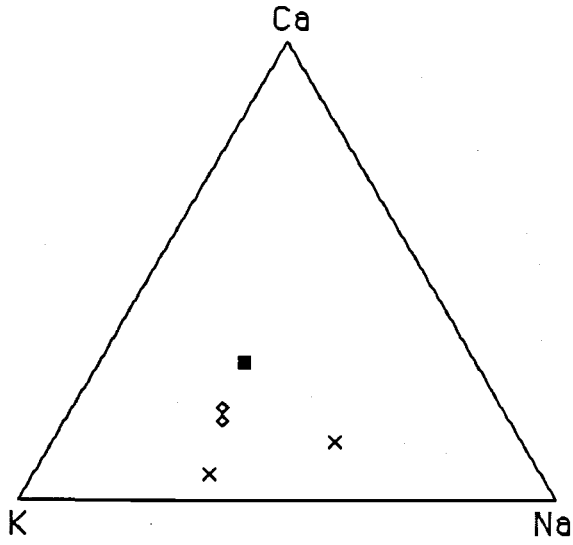

Fig. 15. Ca-K-Na diagram of Lahor granitic complex.

◇ Shang granite
■ Dubair granite
× Shorgara pegmatite

The compatible group elements include chromium, cobalt, and scandium. The compatible group elements differ from the K-group elements in that they tend to concentrate in the ferromagnesian minerals. Chromium content in the Besham gneisses varies from 1.8 to 3.5 ppm, with no distinctive trend separating the quartzofeldspathic gneiss from the sodic quartzofeldspathic gneiss. The concentration of cobalt is 0.8 to 1.2 ppm. Scandium varies from 1.3 to 7.8 ppm.

The thorium group includes thorium and uranium. Sample #108, a quartzofeldspathic gneiss, has very high thorium content (55 ppm), while the other Besham gneisses vary from 1.7 to 7 ppm (Figs. 9 and 10). Thorium is enriched in the quartzofeldspathic gneiss relative to average Archean upper crust. Conversely, thorium is generally depleted in the sodic quartzofeldspathic gneiss relative to average Archean upper crust. Uranium content varies from 2.3 to 7.0 ppm.

The high field strength elements include zirconium, hafnium, and tantalum. These elements have high charge/ionic radius and are not incorporated into most of the common minerals. The ratio of Zr/Hf for the Besham gneisses is consistently 32 to 35. The spider diagram in figure graphically demonstrates the systematic positive correlation of zirconium and halfnium to each other in the Besham gneisses. The concentration of tantalum varies from 0.3 to 1.4 ppm.

The rare earth elements include La, Ce, Nd, Sm, Eu, Tb, Yb, and Lu. REE plots for the Besham gneisses are presented in Figure 17. The chondrite normalized (Anders and Ebihara, 1982) rare earth element pattern of the sodic quartzofeldspathic gneiss samples shows that two of the sodic quartzofeldspathic gneisses (#052 and #043b) are enriched when compared

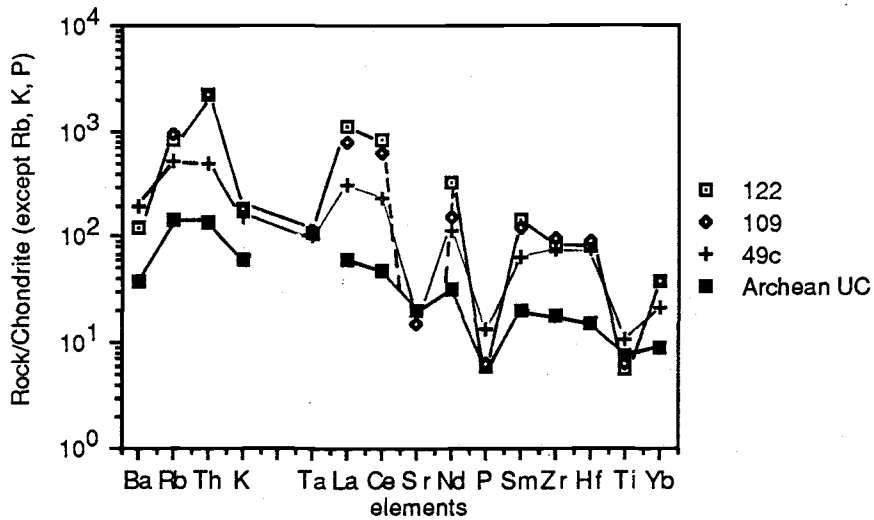

Fig. 16. Spidergrams for the Shang granite (122 and 109) and Dubair granite (49c). Archean upper crust from Taylor and McClennan, 1985.

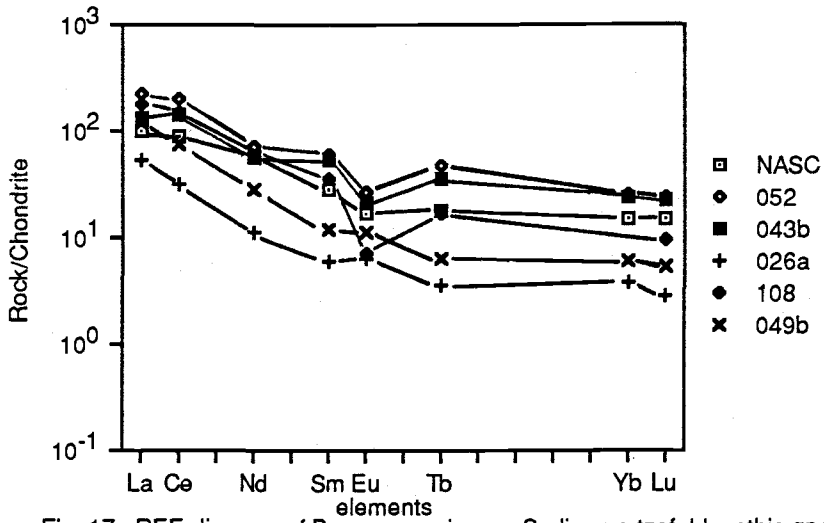

Fig. 17. REE diagram of Besnam gneisses. Sodic quartzofeldspathic gneiss (052, 043b, 026a), quartzofeldspathic gneiss (108, 049b), and NASC (from Haskin et al., 1968).

with the North American Shale Composite (N.A.S.C.), and one (#026a) is not enriched. The composition of average North American shale is thought to represent the average chemical composition of the earth's upper continental crust (Haskin *et al.*,, 1968). Compared with C1 chondrite, most materials at or near the earth's surface are enriched in the REE, for example, the N.A.S.C. The same two enriched sodic quartzofeldspathic gneisses also display a negative Eu anomaly, which indicates that plagioclase fractionated from the protolith or was a residual phase in the source area. The third sodic quartzofeldspathic gneiss, however, displays a slightly positive Eu anomaly.

Most evolved protoliths are more enriched in the light rare earth elements (LREE) than in the heavy REE (HREE), as shown by a high ratio of La/Lu for chondrite normalized (cn) abundances. The average La/Lu(cn) of the two sodic quartzofeldspathic gneisses is 7.6, *versus* 6.8 for N.A.S.C.. La/Lu(cn) for the third sodic gneiss is 18.9, which is similar to the average value of 20.9 for the quartzofeldspathic gneisses.

One quartzofeldspathic gneiss (#108) has a strong, negative Eu anomaly, while the other (#049b) has a slightly positive Eu anomaly and a lower overall concentration of REE relative to N.A.S.C., in particular a depletion of HREE.

Trace elements in the amphibolite Chondrite normalized spidergrams for the amphibolite are shown in Figure 13. The incompatible element data for this plot have been "double-normalized" to Yb(n)=10 after Thompson *et al.* (1984). This convention makes incompatible element patterns of basic rocks easier to compare. In addition, the international standard basalt BHVO-1 is plotted for comparison.

The K-group elements in the amphibolite are enriched 2 to 3X relative to BHVO-1. Rubidium concentrations in the amphibolite are in the range of 19 to 34 ppm, with K/Rb ratios consistently 111 to 143. Cesium and barium concentrations are below detectable limits for two of the four amphibolites analyzed. For the other two amphibolites, cesium is 0.5 to 0.9 ppm, and barium is 558 ppm in sample #12b.

The compatible elements are enriched in the amphibolite. Chromium ranges from 79 to 188 ppm, cobalt from 31 to 53 ppm, and scandium from 37 to 47 ppm.

Thorium in the amphibolite ranges from 2.2 to 2.7 ppm. Ternary plots of Th-Hf/3-Ta are utilized to discriminate tectonic setting for rocks of basaltic composition (Fig.18)(Wood *et al.*, 1979). The amphibolite of the Besham area is consistent with a volcanic arc basalt. Uranium concentrations are below detectable limits for all four amphibolite samples analyzed.

The high field strength elements in the amphibolite are depleted relative to BHVO-1. The spider diagram also shows a peak at zirconium. Zr/Hf ratios are high, ranging from 58 to 95.

The REE pattern of the Besham area amphibolite shows a LREE enrichment at 20-25 times chondrite, a HREE enrichment of 10 times chondrite, and a relatively flat pattern with average (La/Lu)cn = 2.7 (Fig. 19). The pattern is typical of rocks with island arc affinities.

Trace elements in the Lahor granitic complex The K-group elements in the Lahor granitic complex are enriched relative to average Archean upper crust, except strontium, which has a similar concentration to upper crust (Figs. 16 and 20). Rubidium concentration in the Shang and Dubair granites

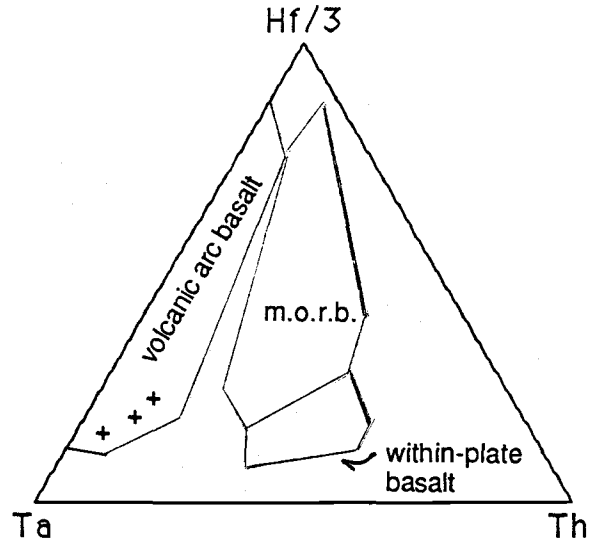

Fig.18. Th-Hf/3-Ta tectonic discrimination diagram for amphibolites. Plot after Wood *et al.*, 1979.

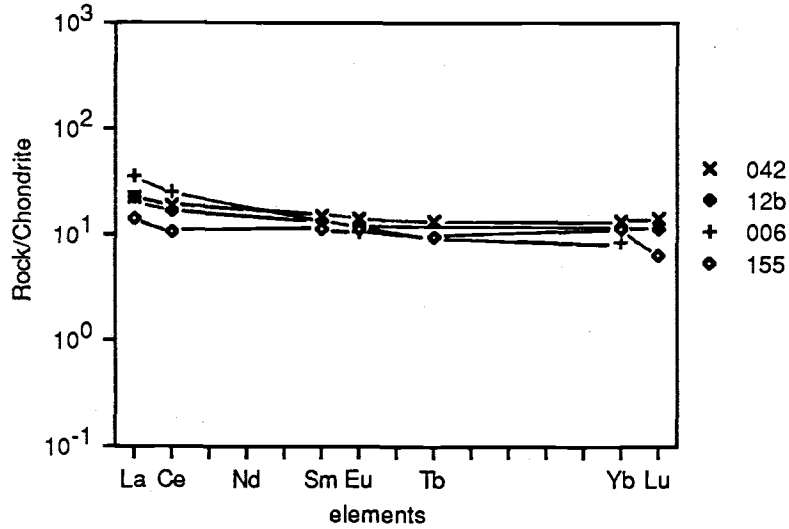

Fig. 19. REE diagram of amphibolites (042,12b,006, and 155).

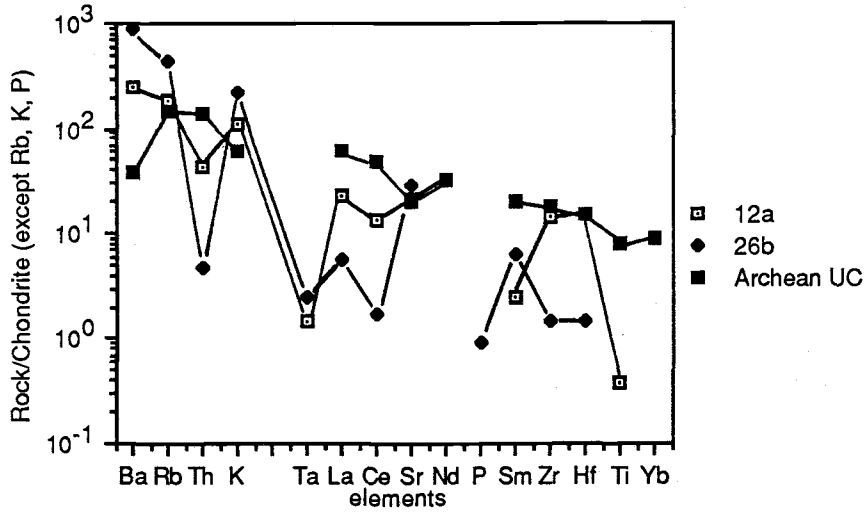

Fig. 20. Spidergrams for Shorgara pegmatite. Archean upper crust from Taylor and McClennan, 1985.

is 179 to 316 ppm. Rubidium is variable in the Shorgara pegmatite at 64 and 151 ppm.

Cesium content is 3 to 5 ppm in the Shang and Dubair granites, and 1 ppm in Shorgara pegmatite. Barium is extremely enriched (6100 ppm) in the more sodic of the two pegmatites (#26b).

The compatible group elements have concentrations in the Lahor granitic complex typical for granitic rocks, with the more mafic rocks containing more compatible elements. Chromium values range from 5 to 6 ppm in the Shang and Dubair granites to 1.3 in the Shorgara pegmatite. The fact that scandium, like chromium and cobalt, is preferentially crystallized in the lattice of mafic minerals is evident from the scandium concentration of 7 to 12 ppm in the Shang and Dubair granite, respectively, and only 0.1 to 0.6 ppm in the Shorgara pegmatite.

Thorium concentration displays a positive peak of enrichment at 1300x chondrite for Shang granite, and 500x chondrite for Dubair granite.Shorgara pegmatite demonstrates the opposite characteristic, *i.e.*; a negative trough for thorium. Uranium values in the Shang and Dubair granite are 5 to 10 ppm; uranium was below detectable limits in the sampled pegmatites.

Concentrations of the high field strength elements are consistent within the Shang and Dubair granite (Zr/Hf= 35, Ta = 2 ppm), but less consistent within the Shorgara pegmatite (Zr/Hf= 31 and 150, Ta = .04). These trends can be seen on their respective spider diagrams.

The REE plot of the Lahor granitic complex shows that the Shang and Dubair granite are extremely enriched relative to C1 chondrite in all the REE and have a large, negative Eu anomaly, while the Shorgara pegmatite is

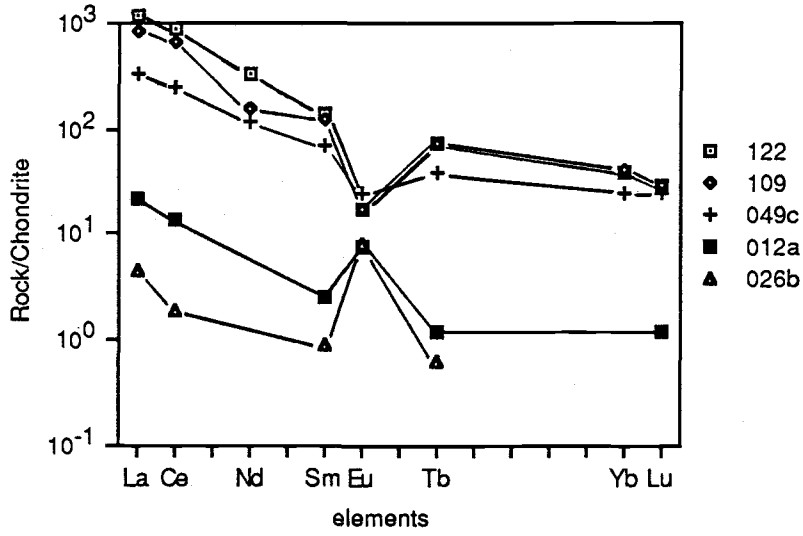

Fig. 21. REE diagram of Lahor granitic complex. Shang granite (122 and 109), Dubair granite (049c), and Shorgara pegmatite (012a and 026b).

only slightly enriched in REE and demonstrates a large positive Eu anomaly (Fig. 21). The average (La/Lu)cn for the highly fractionated and evolved Shang Granite is 35, whereas the ratio is 11.6 for the pegmatite.

Trace elements of the tourmaline granite and the leucogranite The tourmaline granite is a boulder deposited in the Karora group metaconglomerate. The tourmaline granite has high concentrations of the K-group elements (Fig. 22), a high ratio of Zr/Hf=77, low compatible element content, and low thorium and uranium (0.7 and 1.0, respectively). The REE plot (Fig. 23) shows LREE enrichment at La/Lu (cn) = 110, and a slight negative Eu anomaly is present.

The leucogranite has high concentrations of the K-group and Th-group elements, low compatible element content and Zr/Hf= 38. The REE plot for the leucogranite shows LREE enrichment of 10-100 times chondrite, an indistinct negative Eu anomaly, a relatively flat pattern of HREE enrichment of 10 times chondrite, and La/Lu (cn) = 31.

Trace elements of the Mansehra and Choga granites The K-group, the Th-group, and the compatible elements are enriched in the Mansehra granite relative to average Archean upper crust, as seen on the spider diagram presented in Figure 24. The high field strength elements are enigmatic, with an unusually low Zr/Hf ratio of 0.4. Tantalum concentration is 2 ppm. The REE plot of the Mansehra granite demonstrates a remarkable correlation of the Mansehra granite to the N.A.S.C. Since N.A.S.C. represents the average composition of continental crust, the REE data complements previous studies by suggesting that the Mansehra pluton derived a major magmatic contribution from continental crustal material.

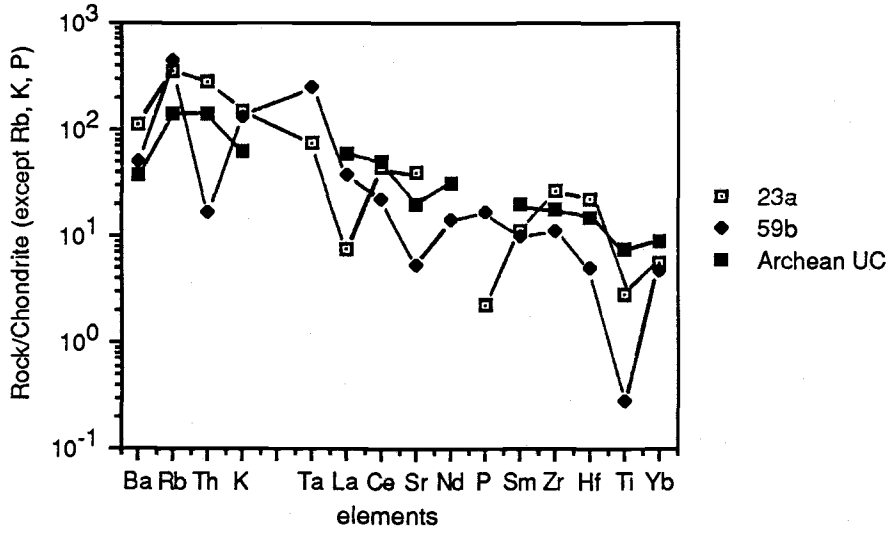

Fig. 22. Spidergrams for leucogranite (23a) and tourmaline granite (59b). Archean upper crust from Taylor and McClennan, 1985.

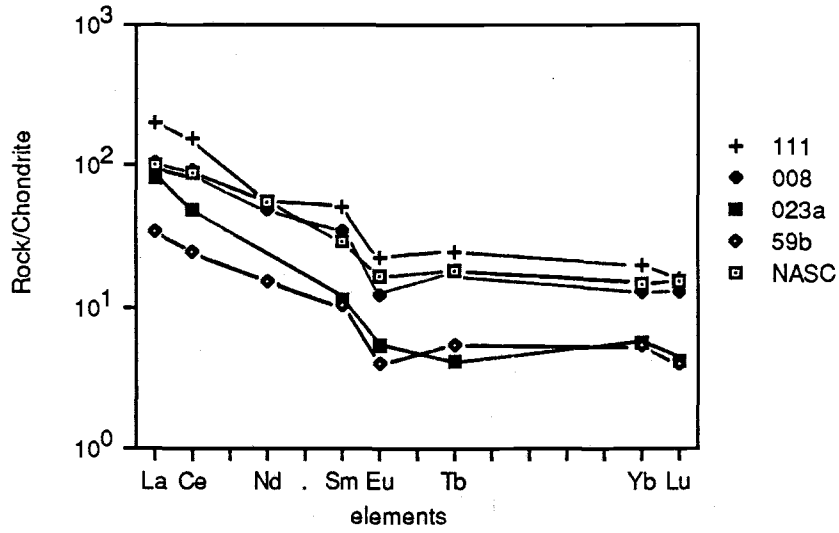

Fig. 23. REE diagram of Choga granite (111), Mansehra granite (008), leucogranite (023a), tourmaline granite (059b), and NASC (from Haskin et al., 1968).

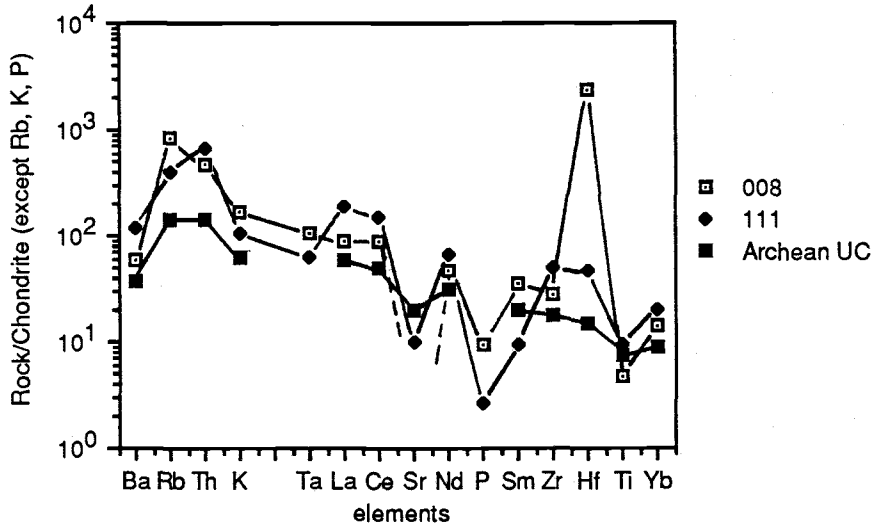

Fig. 24. Spidergrams for Mansehra granite (008) and Choga granite (111). Archean upper crust from Taylor and McClennan, 1985.

Choga granite is enriched in all the K-group elements relative to average Archean upper crust except strontium (Fig. 24). It is also enriched in the Th-group and the compatible elements. The ratio Zr/Hf = 38, and tantalum content is 1.3 ppm. The REE plot for Choga granite shows significant LREE enrichment averaging 180 times chondrite, a slight negative Eu anomaly, and a flat HREE pattern at 20 times chondrite (Fig. 23). The ratio of (La/Lu)cn = 13. The REE pattern for the Choga granite mimics the patterns for Mansehra granite and N.A.S.C., but is slightly enriched relative to them.

DISCUSSION

The Besham uplift has exposed basement rocks that are significantly different from any of the other plutonic and metamorphic rocks of southern Kohistan and that are not seen elsewhere in the Pakistan Himalaya west of the Nanga Parbat-Haramosh Massif (NPHM). Field, petrographic and geochemical evidence suggests a complex geological history for the Besham area.

The oldest rocks within the Besham area basement uplift are the quartzofeldspathic gneiss and sodic quartzofeldspathic gneiss of the Besham group. These quartzofeldspathic paragneisses are peraluminous. The scatter seen in the major element data, particularly in sodium and potassium (Fig. 6) for the Besham gneisses may be due to variability in the composition of the sedimentary protoliths of the gneisses.

The sedimentary protoliths of the Besham group gneisses may have been metamorphosed *in situ*. (Butt, 1983) at a depth slightly shallower than the depth at which granite melting would occur for that particular geothermal gradient. Evidence for this includes the highly variable texture of the gneisses, which in places is migmatitic, with moderately gneissic fabric in the same outcrop. Furthermore, there are no large scale igneous emplacement features that would indicate that the Besham gneisses are orthogneiss, or that the gneisses are plutonic in scale, as proposed by Ashraf *et al.*, (1980).

Figure 14 shows Fe_2O_3 + MgO plotted against Al_2O_3/SiO_2 to distinguish tectonic setting in which the protolith sedimentary rocks of the Besham gneisses were deposited (Bhatia, 1983). Fields are derived from Paleozoic rocks of known tectonic setting. The most likely environment appears to be associated with Bhatia's (1983) "active continental margin"

field, which is consistent with known geologic constraints. This field includes sediments derived from siliceous volcanic rocks or granitic gneisses of uplifted basement that are deposited in marginal retro-arc or pull apart basins.

The Besham gneisses may be correlative to the Nanga Parbat gneisses (Butt, 1983). Both are metamorphic and granitic terrains, and both occur within structural basement highs along the northern margin of the Indian plate. Geochemical data also allow this correlation.

The second-oldest rocks of the Besham area are mafic dikes that intruded the sedimentary protoliths of the Besham group. The sedimentary rock protoliths were later metamorphosed into the Besham group gneisses and metasediments, and the mafic dikes into amphibolites.

The protolith for the amphibolite bodies found within the Besham area basement uplift is classified as tholeiitic based on its major element oxides content, as shown on four separate diagrams (Figures 8, 11, 12, and 14). Field evidence indicating a protolith for the amphibolite was ambiguous, however, and marl was considered to be a potential protolith. This ambiguity was largely due to the transposition of bedding that formed tectonic lenses, pods and boudins in most of the pre-Karora group rocks, thereby disguising cross-cutting relationships.

Trace and major element analyses of the amphibolite suggest that the protolith was tholeiitic, not sedimentary. For example, the concentration of compatible elements (Cr, Co and Sc) are high in the amphibolite. Chromium in the amphibolite varies from 79 to 188 ppm, which is 2 to 5x higher than values reported for sedimentary rocks (Wedepohl, 1978) that could be metamorphosed to produce an amphibolite. Cobalt concentration

in the amphibolite is also about 2x higher than values expected for potential sedimentary protoliths.

Trace element abundances may also serve as discriminators of tectonic setting. For example, the REE plot of the Besham area amphibolites is typical of rocks with island arc affinities (Fig. 19). A tectonic discrimination diagram of Th-Hf/3-Ta for the amphibolite is also consistent with a volcanic arc basalt (Wood *et al*, 1979). Island arc affinities, however, are not particularly consistent with known constraints on the tectonic setting of the Besham area uplift, such as the location of the uplift within a thick sequence of rocks with continental affinities. Continental rift basalt is consistent with the known tectonic constraints, and might be a reasonable protolith for the amphibolite. Indeed, values for chromium reported from African rift basalts (Wedepohl, 1878) are similar to chromium concentrations in the amphibolite.

The ratio K/Rb may be used as another tectonic disriminator for the amphibolite. K/Rb in the amphibolite ranges from 111 to 143. These values, however, are 0.5x less than values reported for African rift basalts (Wedepohl, 1978).

Geochemical evidence allows, therefore, that the protolith of the amphibolite has volcanic island arc affinities. Furthermore, REE signatures of some mafic dikes in the Nanga Parbat gneiss (Verplanck, 1986) are similar to signatures of amphibolites from the Besham area basement uplift.

Field and geochemical evidence suggests that Shang granite, Dubair granite and Shorgara pegmatite are comagmatic. Both the Shang and Dubair are peraluminous granites that intrude the Besham group gneisses and metasediments, and both contain abundant blue-grey microcline. Shorgara pegmatites intrude all the pre-Karora group rocks of the Besham

area basement uplift except the Shang and Dubair granites. Shorgara pegmatite is found only at the margins of the Shang and Dubair granites, and their abundance rapidly diminishes towards the centers of the plutons.

The spidergrams for Shang and Dubair granites resemble other "S-type" granites (Fig. 16)(Thompson *et al.*, 1984). The systematic downward slope from left to right and the strong, negative troughs at strontium, phosphorous, and titanium are common characteristics of granites derived from sediments.

On a Q-A-P ternary diagram the Shang and Dubair granites plot in a tight cluster with the Besham granite gneiss, thus the sedimentary protolith of the Shang and Dubair granites may be the same sedimentary protolith from which the Besham gneisses formed (Fig. 7). At some depth below where sedimentary rocks were being metamorphosed into Besham gneisses, melting of the sedimentary protolith might have occurred. This melt might then have migrated upwards into the overlying Besham gneisses and metasediments as a small intrusion. Pegmatites associated with the small intrusion would cross-cut all units of the Besham group.

REE plots of the Shang and Dubair granite (Fig. 21) and the Besham gneisses (Fig. 17) allow the above hypothesis as a model of the relationship between the Lahor granitic complex and the Besham group. A magma with the REE signature of sample #49c could represent the composition of the early melt. The slight positive Eu anomaly progressively became a strong negative anomaly as first melts gave way to melts dominated by potassic feldspar rather than calcic feldspar. REE-enriched sample #122 could represent the end member of the system. The REE signature of the Shorgara pegmatite is also shown on Figure 21. Potassium feldspar may be

responsible for the Eu peak observed in the REE plot of the pegmatite (Gromet and Silver, 1983).

Although it is difficult to provide irrefutable evidence for more than one metamorphic event in the Besham area uplift, there are indications that two metamorphic events may have occurred. The unconformity above the Besham group, amphibolite, and Lahor granitic complex may separate rocks that have been metamorphosed more than once from rocks that were subjected to only one metamorphic event. Based on field and petrographic evidence, the Karora group has been metamorphosed to middle greenschist facies. This most recent event masks vestiges of earlier events, however, the sediments that comprised the protolith of the Besham gneisses and the Lahor granitic complex were probably metamorphosed to epidote-amphibolite facies before deposition of the Karora group. The evidence for a pre-Karora group metamorphic event includes the presence of clasts of the Besham gneiss and Shang granite (which is foliated) deposited within the Karora group conglomerate. It is probable that this foliation existed before the clasts were deposited in the conglomerate. Furthermore, pre-Karora group lithologies all demonstrate some degree of tectonic disruption and boudinage. The Karora group apparently has not been subjected to this degree of deformation, as lateral continuity of units is more common in the Karora group than in pre-Karora group lithologies.

The leucogranite is a previously unrecognized unit that intrudes both the Besham group and the Karora group in very small sills. The leucogranite is relatively undeformed and unmetamorphosed. There are no leucogranitic dikes associated with the sills.

The Mansehra and Choga granites help constrain the geologic setting of the Besham area basement uplift. The Mansehra granite is a 516 ± 16 m. y. (LeFort *et al.*, 1980) peraluminous granite that is cut by the fault zone that bounds the eastern side of the uplift, therefore the uplift and the rocks within it are probably older than the Mansehra granite. The REE plot of the Mansehra granite demonstrates a remarkable correlation of the Mansehra granite to the N.A.S.C. (Fig. 23). Since N.A.S.C. represents the average composition of continental crust, the REE data complements previous studies by suggesting that the Mansehra pluton derived a major magmatic contribution from continental crustal material.

The Swat granite gneiss is a suite of porphyritic granites that is similar to the Mansehra granite and is exposed in the lower Swat region, west of Besham (Martin *et al.*, 1962; King, 1964). The age of the Swat granite gneiss is not known, but it is thought to be similar to the age of the Mansehra granite (Lawrence *et al*, 1988). The oldest unit of the Swat granite gneiss, the Choga granite, crops out 10 km west of Karora, west of the fault zone that bounds the Besham area basement block. The REE pattern for the Choga granite mimics the patterns for Mansehra granite and N.A.S.C., but is slightly enriched relative to them (Fig. 23).

CONCLUSIONS

(1) The Besham gneisses were formed from sedimentary protoliths.

(2) The Besham gneiss and the Lahor granitic complex may have been formed during a regional metamorphic event from the same sedimentary protolith.

(3) Variable protolith composition may be responsible for the bimodal chemistry of the Besham group quartzofeldspathic and sodic quartzofeldspathic gneisses.

(4) Mafic dikes that intrude the pre-Karora group rocks are tholeiitic and have island arc affinities.

(5) There is evidence for more than one metamorphic event in pre-Karora group rocks.

(6) Young leucogranitic sills are a previously unrecognized unit. They are the youngest rocks recognized in the study area.

(7) Gneisses and amphibolites of the Besham area basement uplift may be correlative to Nanga Parbat gneisses and mafic dikes, respectively.

REFERENCES

Anders, E., and Ebihara, M., 1982, Solar-System abundances of the elements: Geochemica et Cosmochemica Acta, v. 46, p. 2363-2380.

Ashraf, M., Choudhry, M.N. and Hussain, S.S., 1980, General geology and economic significance of the Lahor granite and rocks of southern ophiolite belt in Allai-Kohistan area: Proceed. Intern. Comm. on Geodynamics, Spec. Issue, Geol. Bull. Univ. Peshawar, v. 13, p. 207-213.

Bhatia, M.R., 1983, Plate tectonics and geochemical composition of sandstones: Jour. of Geol., v. 91, p. 611-627.

Butt, K.A., 1983, Petrology and geochemical evolution of Lahor pegmatoid/granite complex, northern Pakistan, and genesis of associated Pb-Zn-Mo and U mineralization, in: Granites of the Himalayas , Karakoram and Hindu Kush, (F.A. Shams, ed.), Institute of Geology, Punjab University, Lahore,Pakistan, p. 309-326.

Calkins, J.A., Offield, T.W., Abdullah, S.K.M., and Ali, S.T., 1975, Geology of the southern Himalayas in Hazara: U.S.G.S Prof. Paper 716-C, 29 p.

Chaudhry M.N., Ashraf, M., Hussain, S.S., 1983, Lead-zinc mineralization of Lower Kohistan District, Hazara Division, NW Frontier Province, Pakistan: Kashmir Jour. of Geol., v. 1, no. 1, p. 31-37.

Coward, M.P., Jan, M.Q., Rex, D., Tarney, J., Thirwall, M., and Windley, B.F., 1982, Geotectonic framework of the Himalaya of N. Pakistan: Jour. Geol. Soc. London, v. 139, p. 299-308.

Fletcher, C.J.N., Leake, R.C., and Haslam, H. W., 1986, Tectonic setting, mineralogy and chemistry of a metamorphosed stratiform base metal deposit within the Himalayas of Pakistan: Jour. Geol. Soc., London, v. 143, p.521-536.

Gregg, J.M., and Sibley D.F., 1984, Epigenetic dolomitization and the origin of xenotopic dolomite texture: Jour. Sed. Pet., vol. 54, no. 3, p. 908-931.

Gromet, L.P., and Silver, L.T., 1983, Rare earth element distributions among minerals in a granodiorite and their petrogenetic implications: Geochemica and Cosmochemica Acta, v. 47, p. 925-939.

Haskin, L.A., Haskin, M.A., Frey, F.A., and Wildeman, T.R., 1968, Relative and absolute terrestrial abundances of the rare earth elements, in: Origin

and Distribution of Elements, (Ahrens, L.H., ed.), Pergamon, Oxford, p. 889-912.

Irvine, T.N., and Baragar, W.R.A., 1971, A guide to the chemical classification of the common volcanic rocks: Canadian Jour. Earth Sci., v. 8, p. 523-548.

Jacob, K. H., and Quittmeyer, R.C., 1979, The Makran Region of Pakistan and Iran: trench-arc system with active plate subduction, in: Geology of Pakistan, (Farah and DeJong, eds), Geol. Survey Pakistan, Quetta, Pakistan.

Jan, M.Q., and Tahirkheli, R.A.K., 1969, The geology of the lower part of Indus Kohistan (Swat), West Pakistan: Geol. Bull. Univ. Peshawar, v. 4, p. 1-13.

Jan, M.Q., 1977, The Kohistan basic complex, a summary based on recent petrological research: Geol. Bull. Univ. of Peshawar, v. 9-10, p. 36-42.

Jan, M.Q., 1980, Petrology of the obducted mafic and ultramafic metamorphites from the southern part of the Kohistan island arc sequence, Geol. Bull. Univ. Peshawar, v. 13, p. 95-107.

Klootwijk, C.T., Conaghan, P.J., and Powell, C., 1985, The Himalayan Arc: large-scale continental subduction, oroclinal bending and back-arc spreading: Earth Planet. Sci. Lett., v. 75, p. 167-183.

King B.H., 1964, The structure and petrology of part of Lower Swat, West Pakistan, with special reference to the origin of granite gneisses: unpublished Ph. D. thesis, Univ. of London, 130 p.

Laul, J.C., 1979, Neutron activation analysis of geological materials: Atomic Energy Review., v. 17, p. 603-695.

Lawrence, R.D., and Ghauri, A.K., 1983, Observations on the structure of the Main Mantle Thrust at Jijal, Kohistan, Pakistan: Geol. Bull. Univ. Peshawar, v. 16, p. 1-10.

Lawrence, R.D., Kazmi, A.H., and Snee, L.W., 1988, in press, in: Emeralds of Pakistan: Geology, Gemology, and Genesis, (A.H. Kazmi and L.W. Snee, eds.), Van Nostrand Reinhold, N.Y.,N.Y.

Lawrence, R.S., Khan, S.H., DeJong, K.A., Farah, A., and Yeats, R.S., 1981, Thrust and strike slip fault interaction along the Chaman transform zone, Pakistan: Geol. Soc. London Spec. Publ. 9, p. 363-370.

LeFort, P., Debon, F., Sonet, J., 1980, The "Lesser Himalayan" cordierite granite belt, typology and age of the pluton of Mansehra, Pakistan, Geol. Bull. Univ. Peshawar, v. 13, p. 51-62.

Madin, I., 1986, Structure and neotectonics of the northwestern Nanga Parbat-Haramosh Massif: unpublished M.S. thesis, Oregon State University, 160 p.

Martin, N.R., Siddiqui, S.F.A., and King, B.H., 1962, A geological reconnaissance of the region between the lower Swat and Indus Rivers of Pakistan: Geological Bulletin Punjab University, v. 2, p. 1-14.

Molnar, P., 1986, The geologic history and structure of the Himalaya: American Scientist, v. 74, p.144-154.

Molnar, P., and Tapponnier, P., 1975, Cenozoic tectonics of Asia: effects of a continental collision: Science, v. 189, p. 419-426.

Miyashiro,A., 1974, Volcanic rock series in island arcs and active continental margins: Am. Jour. Sci., v. 247, p. 321-355.

Nockolds, S.R., 1954, Average chemical composition of some igneous rocks: Bull. Geol. Soc. Am., v. 66: 1007-1032.

Powell, C.McA., 1979, A speculative tectonic history of Pakistan and surroundings: some constraints from the Indian Ocean, in: Geodynamics of Pakistan (A. Farah and K.A. DeJong, eds.), Geol. Survey Pakistan, Quetta, Pakistan, p. 5-24.

Seeber, L., Armbruster, J.G., and Quittmeyer, R.C., 1981, Seismicity and continental subduction in the Himalayan arc, in: Zagros, Hindu-Kush, Himalaya, Geodynamic Evolution, AGU Geodynamics Series, (H.K. Gupta and F.M. Delany, eds.) v. 3, p. 215-242.

Sengor, A.M.C., 1979, Mid-Mesozoic closure of Permo-Triassic Tethys and its implications: Nature, v. 279, p. 590-593.

Sun, S.S., 1980, Lead isotopic study of young volcanic rocks from mid-ocean ridges, ocean islands and island arcs: Phil. Trans. Royal Soc. London, Series A, v. 297, p. 409-445.

Streckeisen, A., 1976, To each plutonic rock its proper name: Earth Sci. Review., v. 12, p. 1-33.

Taggart, J.E., and Wahlberg, J.S., 1980, New mold design for casting fused samples: Advances in x-ray analysis, v. 23, p. 257-261.

Taggart, J.E., and Wahlberg, J.S., 1980, A new in-muffle automatic fluxor designed for casting glass discs for x-ray fluorescence analysis: Federation Analytical Chemists and Spectroscopies Soc. Meeting, Philadelphia, PA., Sept. 1980.

Taggart, J.E., Lichte, F.E., and Wahlberg, J.S., 1981, Methods of analysis using x-ray fluorescence and induction-coupled plasma spectroscopy: U.S.G.S. professional paper 1250, p. 683-687.

Tahirkheli, R.A.K., 1982, Geology of the Himalaya, Karakoram, and Hindu Kush in Pakistan: Geol. Bull. Univ. Peshawar, v. 15, 51 p.

Tahirkheli, R.A.K., and Jan, M.Q., 1979, A preliminary geological map of Kohistan and adjoining areas, N. Pakistan, 1:1,000,000: Geol. Bull. Univ. Peshawar, v. 11.

Taylor, S.R., and McClennan, S.M., 1985, The Continental Crust:; its composition and evolution, (A. Hallam, ed.), Blackwell Scientific Publications, Palo Alto, CA., 312 p.

Verplanck, P.L., 1986, A field and geochemical study of the boundary between the Nanga Parbat-Haramosh Massif and the Ladakh Arc terrane, northern Pakistan: unpublished MS thesis, Oregon State University, 136 p.

Wedepohl, K.H., 1978, Handbook of Geochemistry, v. 2, Springer-Verlag, New York, NY.

Wood, D.A., Joron, J.L., Treuil, M., 1979, A reappraisal of the use of trace elements to classify and discriminate between magma series erupted in different tectonic settings: Earth Planet. Sci. Lett., v. 45, p. 326-336.

Yeats, R.S., and Lawrence, R.D., 1984, Tectonics of the Himalayan thrust belt in northern Pakistan, in: Marine Geology and Oceanography of Arabian Sea and Coastal Pakistan (B.U. Haq and J.D. Milliman, eds.), Van Nostrand Reinhold, p. 177-198.

Yeats, R.S., and Hussain, A., 1987, Timing of structural events in the Himalayan foothills of northwestern Pakistan: G.S.A. Bull., v. 99, p. 161-176.

Zeitler, P.K., Johnson, N.M., Naesser, G.W., and Tahirkheli, R.A.K., 1982, Fission-track evidence for Quaternary uplift of the Nanga Parbat region, Pakistan: Nature, v. 298, p. 255-257.